Basin Research (2004) **16**, 1–24, doi: 10.1111/j.1365-2117.2003.00223.x

Evolution of the Himalayan foreland basin, NW India

Yani Najman,* Kit Johnson,† Nicola White‡ and Grahame Oliver§

**Department of Environmental Science, Lancaster University, Bailrigg, Lancaster LA1 4YQ, UK*
†Fission Track Research Group, Department of Geological Sciences, University College London, Gower St., London, UK
‡Department of Earth Sciences, Cambridge University, Downing St., Cambridge CB2 3EQ, UK
§School of Geography and Geosciences, Purdie Building, University of St Andrews, St Andrews, Fife KY16 9ST, UK

ABSTRACT

This paper provides new information on the evolution of the Himalayan foreland basin in the under-reported region of the Kangra and Subathu sub-basins, NW India. Comparisons are made with the better documented co-eval sediments of Nepal and Pakistan to build up a broader picture of basin development. In the Subathu sub-basin, shallow marine sediments of the Palaeocene–lower Lutetian Subathu Formation are unconformably overlain by the continental alluvial Dagshai and Kasauli Formations and Siwalik Group. The start of continental deposition is now dated at younger than 31 Ma from detrital zircon fission track data, thereby defining the duration of this major unconformity, which runs basin-wide along strike. Final exhumation of these basin sediments, as thrusting propagated into the basin, occurred by 5 Ma constrained from detrital apatite fission track data. In the Kangra sub-basin, the Subathu Formation is not exposed and the pre-Siwalik sediments consist of the Dharamsala Group, interpreted as the deposits of transverse-draining rivers. In this area, there is no evidence of westerly axial drainage as documented for coeval facies in Nepal. Similar to data reported along strike, facies analysis indicates that the sediments in NW India represent the filled/overfilled stages of the classic foreland basin evolutionary model, and the underfilled stage is not represented anywhere along the length of the basin studied to date.

INTRODUCTION AND GEOLOGICAL SETTING

Peripheral foreland basins form in collisional belts in response to flexural loading of the lithosphere by the adjacent thrust belt (Beaumont, 1981; Jordan, 1981). The traditional description of basin geometry is that of a 'wedge-shaped' basin that deepens towards the hinterland. On the cratonward side, upwarp results in a peripheral forebulge. Propagation of thrusting towards the craton causes cratonward migration of the basin and forebulge. More recently, inclusion of the wedge-top depozone into the foreland basin foredeep-, forebulge- and back-bulge depozone model depicts the basin geometry as a doubly tapered prism (DeCelles & Giles, 1996). The sedimentology, stratigraphy and structure of a foreland basin are, to a large extent, influenced by the tectonics of the orogen. Hence, a detailed knowledge of both mountain belt and basin is required to understand the inter-relationship between the two. In this work, we place constraints on Himalayan foreland basin evolution from an integrated sedimentary facies study and fission track analyses of detrital zircon and apatite from the early Himalayan foreland basin sediments of the Subathu and Kangra sub-basins, Himachal Pradesh, NW India.

Correspondence: Yani Najman, Department of Environmental Science, Lancaster University, Bailrigg, Lancaster LA1 4YQ, UK. E-mail: y.najman@lancaster.ac.uk

The Himalaya formed when the Tethys ocean closed and India and Eurasia collided. The mountain belt consists of six lithotectonic zones, separated by thrust and normal faults (Gansser, 1964) (Fig. 1). From north to south, these belts and their representative rock types are: 1) The Trans-Himalayan zone batholiths, which are interpreted as the Andean-type northern margin of Tethys (Honegger *et al.*, 1982; Coulon *et al.*, 1986; Le Fort, 1996). 2) The Indus Suture Zone, which represents the line of collision between India and Eurasia, and is composed of marine sediments, ophiolites, arc volcanics and melange (Searle, 1983; Garzanti & Van Haver, 1988; Reuber *et al.*, 1987; Reuber, 1989; Robertson & Degnan, 1993). 3) The Tibetan or Tethys Himalayan Zone; these are Cambrian to Palaeocene sediments (the Tibetan Sedimentary Series) deposited on the Indian continental terrace (Fuchs, 1982; Gaetani & Garzanti, 1991). 4) The Greater Himalaya, which is regionally metamorphosed Indian continental crust of mainly Proterozoic age (Parrish & Hodges, 1996; DeCelles *et al.*, 2000) and leucogranites (e.g. Le Fort *et al.*, 1987; Treloar & Searle, 1993 and papers therein). 5) The Lesser Himalaya that is represented by non or weakly metamorphosed Indian continental crust that ranges in age from Proterozoic to Palaeozoic (Valdiya, 1980; Valdiya & Bhatia, 1980; Parrish & Hodges, 1996; DeCelles *et al.*, 2000), and

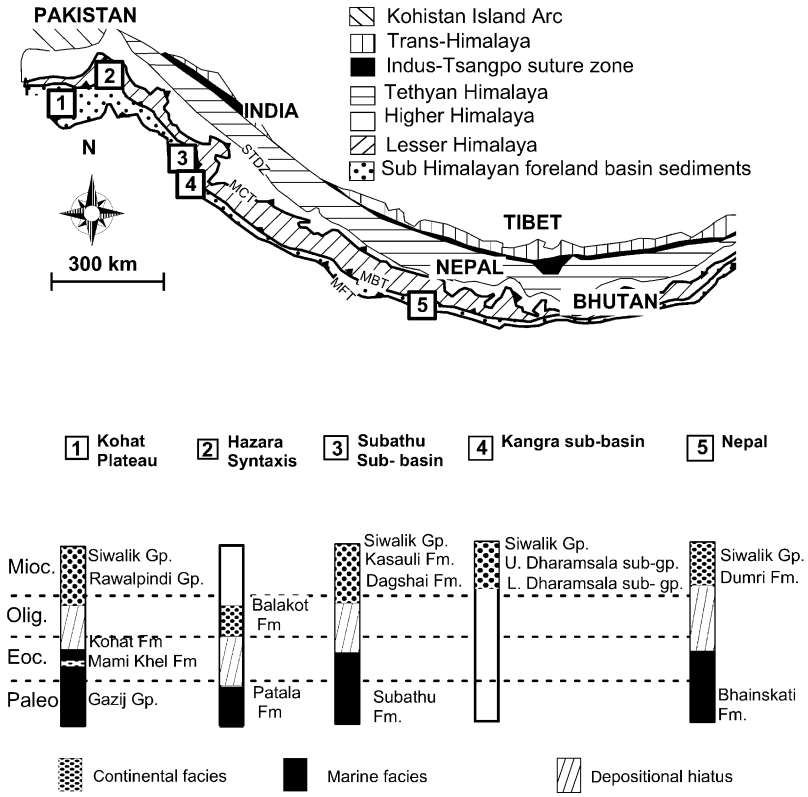

Fig. 1. Simplified geological map of the Himalayan region; boxed numbers refer to stratigraphic sections in the foreland basin, depicted in the lower half of the diagram. Data sources referenced in text. STDZ = South Tibetan Detachment Zone, MCT = Main Central Thrust, MBT = Main Boundary Thrust, MFT = Main Frontal Thrust.

Palaeogene foreland basin sediments (Srikantia & Bhargava, 1967; Srikantia & Sharma, 1970; Sakai, 1989; DeCelles *et al*., 1998a). 6) The Sub-Himalaya, which consists of foreland basin sediments eroded from the rising orogen and deposited in the peripheral foreland basin in front of the mountain belt (Parkash *et al*., 1980; Johnson *et al*., 1985; Harrison *et al*., 1993; Critelli & Garzanti, 1994; DeCelles *et al*., 1998a, b; Najman & Garzanti, 2000; White *et al*., 2001, 2002). The sub-division of the early foreland basin into foredeep, forebulge and back-bulge depozones has been proposed by DeCelles *et al*. (1998a).

The collisional process between India and Eurasia began at approximately 55 Ma (e.g. Rowley, 1996 and references therein, Searle *et al*., 1997; De Sigoyer *et al*., 2000). Subsequent to collision, metamorphism of the Indian crust involved two phases; Eo-Himalayan metamorphism at ca. 40–30 Ma is Barrovian metamorphism of the Greater Himalaya, the result of crustal thickening due to thrust stacking (Prince *et al*., 1999; Vance & Harris, 1999). The climax of Neo-Himalayan metamorphism and production of leucogranite melts at ca. 20 Ma is co-eval with movement along the normal faulting South Tibetan Detachment Zone (STDZ), which defines the northern boundary of the Greater Himalaya, and the Main Central Thrust (MCT), which thrust the Greater Himalaya over the Lesser Himalaya (Staubli, 1989; Searle & Rex, 1989; Metcalfe, 1993). Continued convergence of India with Eurasia resulted in southward propagation of the thrust belt. The Main Boundary Thrust (MBT), which was active in middle–late Miocene or Pliocene (DeCelles *et al*., 1998b; Hodges *et al*., 1988; Meigs *et al*., 1995) times, thrust the Lesser Himalaya over the Sub-Himalaya. The presently active Main Frontal Thrust (MFT) lies to the south of the Sub-Himalaya, and therefore separates it from the present-day foreland basin (Indo-Gangetic plain) to the south (Powers *et al*., 1998).

STRUCTURAL AND STRATIGRAPHIC SETTING OF THE FORELAND BASIN SEDIMENTS, NW INDIA

For India, most workers define the MBT as the thrust separating Lesser Himalayan PreCambrian – Palaeozoic rocks above from Tertiary foreland basin sediments below (e.g. Meigs *et al*., 1995). Thus, apart from a few minor outcrops of Early Tertiary foreland basin sediments outcropping above the MBT (Srikantia & Bhargava, 1967; Srikantia & Sharma, 1970), the foreland basin sediments are located in the Sub-Himalaya. However, it should be noted that some workers (e.g. Loyal, 1990) define the MBT as the thrust boundary between pre-Siwalik foreland basin sediments above and Siwalik foreland basin sediments below, a structural definition similar to that in Nepal (e.g. DeCelles *et al*., 1998a). In India, the Sub-

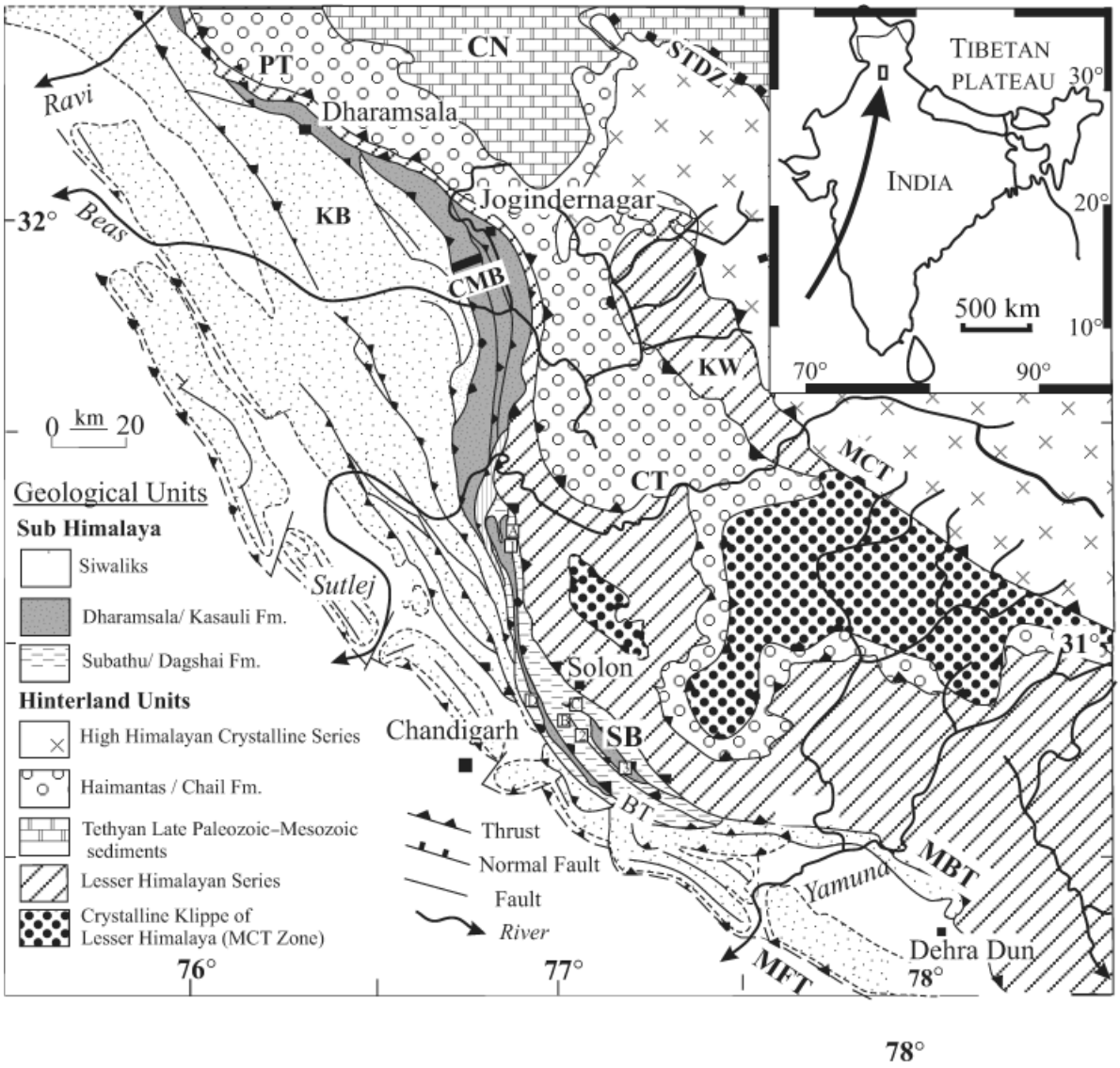

78°

Fig. 2. Geological map of part of the Himalayan orogen and foreland basin in India, showing the location of the Kangra (KB) and Subathu (SB) sub-basins as located in Fig. 1. PT = Panjal Thrust, CT = Chail Thrust, STDZ = South Tibetan Detachment System, MCT = Main Central Thrust, MBT = Main Boundary Thrust, BT = Bilaspur Thrust, MFT = Main Frontal Thrust, KW = Kulu Window, CN = Chamba nappe. Thick line labelled CMB = Chimnun–Makreri–Birdhar section along which the logs shown in Figs 8–12 are located. Boxed numbers: 1 = location of Subathu–Dagshai contact log (Fig. 5); 2 = location of Dagshai Fm Log (Fig. 6); 7 = location of Kasauli Fm log (Fig. 7). Boxed letters: location of samples used for fission track analyses (Table 1); A = Sample Hm96-9A, B = Sample Hm96-17B, C = Hm96-22A, D = Hm96-25B. Map adapted from Karunakaran & Rao (1979), Raiverman *et al*. (1983), Powers *et al*. (1998) and Thakur (1998).

Himalayan foreland basin is subdivided into sub-basins by basement ridges and spurs (Raiverman *et al*., 1983). In this study of NW India, we concentrate on the Early Tertiary succession of the Subathu sub-basin, and adjacent Kangra sub-basin (Figs 1 and 2).

In the Subathu sub-basin, the foreland basin sediments consist of the Palaeogene–E. Miocene Subathu, Dagshai and Kasauli Formations and the Neogene Siwalik Group (Gansser, 1964; Bhatia, 1982) (Fig. 1, column 3). The Subathu Formation is composed of shallow marine facies and consists predominantly of green mudstone with subordinate sandstone and limestone (Mathur, 1978). Uncommon red beds are interbedded in this succession (Mathur, 1979; Najman & Garzanti, 2000). The Dagshai Formation consists of red and grey sandstones, red siltstones and mudstones and caliche. The Kasauli Formation consists of grey sandstones and subordinate mudstones and siltstones, whereas the Siwalik Group is of broadly similar sediment type with the addition of conglomerate. The Dagshai, Kasauli and Siwalik sediments are interpreted as continental deposits.

The Subathu Formation in the Subathu Basin has been dated on the basis of marine fossils as Late Palaeocene–lower Mid-Eocene (Early Lutetian) (e.g. Mathur, 1978; Batra, 1989), although Blondeau *et al*. (1986) recorded an Early Eocene upper age limit for the Subathu Formation to

the west in Jammu, India. Previously, there was debate as to whether the Dagshai Formation overlies the Subathu Formation, either conformably (Bhatia & Mathur, 1965) or unconformably (Wadia, 1975), or whether the Subathu and Dagshai Formations are stratigraphically interlinked (Raiverman & Raman, 1971). Detailed mapping by Batra (1989) and Najman *et al.* (1993) showed that the Dagshai lies above the Subathu Formation, and dating of detrital micas by Najman *et al.* (1997) showed that the majority of the Dagshai Formation was younger than 28 Ma. However, the lowermost part of the Dagshai Formation is mica-free and is therefore undatable by this technique. The current research described here uses an alternative technique, fission track dating of detrital zircons, that shows conclusively the unconformable nature of the Subathu–Dagshai Formation contact. The Kasauli Formation overlies the Dagshai Formation, and has been dated at younger than 28 Ma at two localities and less than 22 Ma at a third, using detrital mica ages (Najman *et al.*, 1997). The contact is conformable and gradual, with a 'transition zone' where the succession resembles the Kasauli Formation sedimentologically, but has greater petrographical resemblance to the Dagshai Formation (Najman & Garzanti, 2000). The contact between the Kasauli Formation and Siwalik Group is not exposed.

The pre-Siwalik strata that outcrop in the Kangra subbasin comprise the lower and upper subgroups of the continental facies Dharamsala Group of Miocene age (Fig. 1, column 4). No Palaeogene marine facies are exposed. Traditionally, the Lower Dharamsala subgroup was further subdivided into the Chimnun, Pabo and Al Formations (Raiverman & Seshavataram, 1965), and the Makreri Formation roughly equivalent to the Upper Dharamsala subgroup (Raiverman *et al.*, 1983). However, more recent work by White *et al.* (2002) has shown that the petrography and Ar–Ar detrital mica ages of the Al Formation are unlike those of the underlying Chimnun and Pabo Formations, but similar to that of the Upper Dharamsala subgroup. Hence, we consider the Al Formation to be the basal unit of the Upper Dharamsala subgroup, overlain by the Makreri Formation.

In contrast to the Subathu Basin, the pre-Siwalik rocks of the Kangra basin have, in general, suffered only limited tectonic disruption and are therefore suitable for extensive sedimentary logging and magnetostratigraphic dating. The exception to this is the base of the Lower Dharamsala subgroup, Chimnun Formation, which is poorly exposed and tectonised and therefore unsuitable for magnetostratigraphic dating. Detrital Ar–Ar muscovite ages from the Chimnun Formation show that the sediments are younger than 21 Ma (on the assumption that the host depositional sediment is younger than the detrital mica ages). This agrees with the minimum age of the formation as determined by the 20-Ma age of the base of the overlying magnetostratigraphically dated sedimentary column. The Pabo Formation is magnetostratigraphically dated at 20–17 Ma, and the overlying Upper Dharamsala subgroup, comprising the Al and Makreri Formations, is magnetostratigraphically dated at 17–13 Ma (White *et al.*, 2001). The Makreri Formation of the Upper Dharamsala subgroup grades conformably into the Lower Siwalik subgroup above. Dharamsala group rocks consist of sandstones, siltstones, mudstones and caliche of interpreted alluvial facies.

DETRITAL GRAIN FISSION TRACK STUDY

Fission tracks result from spontaneous radioactive decay of ^{238}U by fission, causing linear zones of radiation damage in the crystal lattice of the host mineral. This radiation damage is meta-stable, and over a temperature range referred to as the partial annealing zone (PAZ) the crystal lattice reorganises, or anneals, itself. The number of fission tracks in a grain can be related to the time since cooling through the PAZ, whereas the fission track length distribution is related to the temperature and cooling rate, with rapid cooling through PAZ represented by long track lengths of narrow distribution (e.g. Laslett *et al.*, 1987). The PAZ temperature range in apatites is $\sim 60-110\,^{\circ}C$ for time periods of 10^6–10^7 years. These temperatures are typical of those encountered in sedimentary basins with a typical geothermal gradient at a few kilometres depth. Thus apatite data are usually used to constrain post-burial cooling history of basin sediments. In contrast, fission tracks in zircon have a higher resistance to annealing and consequently its PAZ has a higher temperature range than apatite ($\sim$200–320 °C, Tagami *et al.*, 1998). Consequently, post-depositional burial temperatures are unlikely to anneal the fission tracks in zircon, and a record of cooling in the hinterland is preserved in the detrital material.

In this study, one Kasauli Formation sample (Hm96-25B) was analysed for apatite fission track analysis. Three samples were analysed for detrital zircon fission track data; one sample was from the basal Dagshai Formation directly above the Subathu Formation rocks (sample Hm96-9A), one sample was from the Main Dagshai Formation (sample Hm96-17B) and one was from the transition zone between the Dagshai and Kasauli Formations (sample Hm96-22A). Sample locations are shown in Fig. 2. In addition, we performed illite crystallinity, vitrinite reflectance and spore colour measurements on rock samples from these formations in order to determine the post-depositional temperatures to which the detrital minerals had been subjected, and thus better interpret the fission track data.

Fission track results (Table 1)

Figure 3 shows single grain ages presented on radial plots (Galbraith, 1990). The radial plot for sample Hm96-9A shows the data from 10 zircon crystals separated from a basal Dagshai Formation sandstone. The central age is 31 ± 2 Ma. The mean track lengths for this sample are relatively long and the distribution is narrow. Sample Hm96-17B is from the Main Dagshai Formation. Six zircon crystals were analysed that can be separated into two age populations; one population has a central age of 76 ± 6 Ma, and a second population has a central age of 364 ± 45 Ma. The zircons have relatively long mean track lengths with narrow distributions. Sample Hm96-22A is from the Dag-

Table 1. Detrital zircon and apatite fission track results from sediments of the Subathu sub-basin, Himalayan foreland basin, India.

Sample (prefix Hm)	Fm	Mineral and number of crystals	Spontaneous P_s (N_s)	Induced P_i (N_i)	Dosimeter P_d (N_d)	Central FT age Ma ($\pm 1\sigma$)	Relative error %	MCTL* and no. tracks (m)	SD 1σ (m)	Age group 1 Ma ($\pm 2\sigma$)	Age group 2 Ma ($\pm 2\sigma$)
96-9A	Base of Dagshai	Zircon (10)	3.707 (1484)	3.212 (1286)	0.394 (2929)	31.0 ± 1.6	7.8	10.7 ± 0.2 (21)			
96-17B	Dagshai	Zircon (6)	10.91 (2760)	1.166 (295)	0.394 (2729)	239 ± 87	88	10.2 ± 0.3 (32)	1.58	76 ± 6	364 ± 45
96-22A	Dagshai–Kasauli transition†	Zircon (15)	6.947 (2744)	2.343 (295)	0.394 (2729)	49 ± 9	73	10.9 ± 0.3 (35)		29.4 ± 2.2	388
96-25B	Kasauli	Apatite (20)	0.057 (82)	3.550 (5137)	1.853 (12 840)	5.3 ± 0.6	0	14.2 ± 0.6 (40)	1.55		

(i) All track densities (ρ_d, ρ_s and ρ_i) are ($\times 10^6$ t cm^{-2}); number of tracks counted (N) shown in brackets.
(ii) Analyses are by the external detector method using 0.5 for the $4\pi/2\pi$ geometry correction factor.
(iii) Apatite ages calculated using the dosimeter glass CN5 with $\xi_{CN5} = 361 \pm 6$. Zircon ages calculated using dosimeter glass CN2 with $\xi_{CN2} = 137 \pm 2$ (C. Johnson).
(iv) Samples for fission track analyses were prepared using standard separation and polishing techniques. Apatite grains were etched with 5 M HNO_3 at 20 °C for 20 S. Zircon mounts were etched using a binary eutectic melt consisting of KOH and NaOH for times of 4–18 h. Mounts were irradiated with thermal neutrons together with Corning glass dosimeter CN5 for apatite and CN2 for zircons. Counting and track length measurements were carried out under a total magnification of × 1250 with a × 100 dry objective for apatite and oil emersion for zircon. Central ages were calculated by using the International Union of Geosciences Subcommission – recommended zeta calibration approach (Hurford, 1990).
*MCTL = mean confined track length for tracks measured in all grains, or on grains comprising the youngest age group where more than one age population was observed.
†Informally termed the Kumahatti–Solon unit by Najman & Garzanti (2000), these beds sedimentologically resemble the Kasauli Formation but petrographically resemble the Dagshai Formation.

shai–Kasauli transition zone, from which 15 zircon crystals were analysed. Two age populations were identified; the first with a central age of 29.4 ± 2.2 Ma, the second with a central age of 388 Ma. The mean track lengths are long and the distribution is narrow. Hm96-25B is a Kasauli Formation sample from which 20 apatite crystals were analysed. There is a single population aged at 5.3 ± 0.6 Ma, and the mean track length is long and has a narrow distribution. We acknowledge that in some cases, sub-population ages are based on a very small number of grains – however, none of these populations are critical to our resulting interpretations of the duration of basin-wide unconformity or the timing of thrusting in the basin.

Illite crystallinity measurements (Fig. 4)

Kubler (1967), Weber (1972a, b), Kisch (1980a, b) and Aprahamian & Paris (1981) have shown that the width at half height of the 10-Å illite peak on X-ray diffraction patterns decreases with an increase in metamorphic grade as Fe^{2+}, Mg^{2+}, H_2O and OH^- are expelled from the lattice and K^+ is absorbed. This half peak width is known as Hb. To enable better inter-laboratory correlation and to guard against variations in machines, the Weber index (Weber, 1972) is used, whereby crushed quartz is used as an external standard. Hb_{rel} is calculated using the following equation:

$$Hb_{rel} = \frac{Hb(001)illite}{Hb(100)quartz} \times 100.$$

Kubler (1967) used the Hb to define the diagenetic zone (< 200 °C), the anchizone (200–370 °C) and the epizone (> 370 °C). Later, Blenkinsop (1988) calculated that the Hb_{rel} upper and lower limits of the anchizone were 278 and 149, respectively. In this study, we separated and analysed the < 2μm fraction of the rocks in order to measure the diagenetic rather than detrital component and thus obtain an indication of the temperatures to which the rock has been subjected post-deposition. Fig. 4 shows the results, which indicates that the rocks were only subjected to diagenetic to lowest anchizone post-depositional temperatures. These metamorphic conditions would have been sufficient to reset apatite fission tracks, but unlikely to have had a similar effect on fission tracks in zircon.

Vitrinite reflectance and spore colour index (Tables 2 and 3)

Vitrinite reflectance is the percentage of incident light that is reflected from vitrinite. Vitrinite reflectance increases as temperature, pressure and time increase. Barker & Pawlewicz (1986) correlated vitrinite reflectance with maximum palaeotemperature using the equation

$$\ln(R_0) = 0.0096(T) - 1.4,$$

where R_0 is the vitrinite reflectance value and T is the maximum temperature in °C.

Spore and algae change colour from yellow-orange to black as maturation increases. By visually comparing the

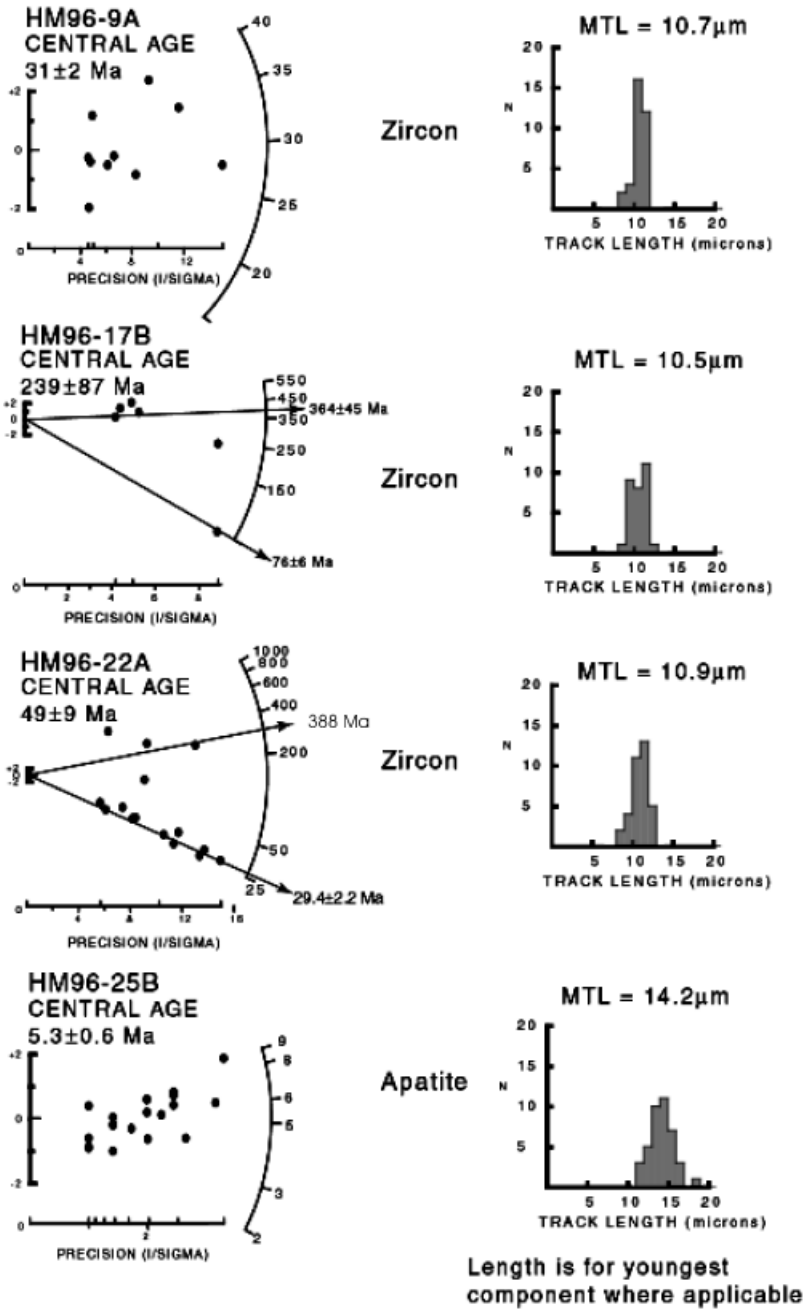

Fig. 3. Radial plots (Galbraith, 1988) showing the spread of individual grain ages within each sample. For radial plots, the position on the *x*-scale records the uncertainty of individual age estimates, whereas each point has the same standard error on the *y*-scale. The further the data point plots from the origin, the more precise the measurement. The radial axis provides the time scale in Ma. The age of each crystal may be determined by extrapolating a line from the origin on the left through the crystal's *x*, *y* co-ordinates to intercept the radial age scale. Sample Hm96-9A = basal Dagshai Formation, Hm96-17B = Dagshai Formation, Hm96-22A = transitional Dagshai–Kasauli Formation, Hm96-25B = Kasauli Formation.

colours of the spores/algae in the sample with a spore colour standard (e.g. Pearson, 1984), an estimation of maturation and a correlation with vitrinite reflectance values can be determined and the palaeotemperature can be calculated.

Samples for this study were prepared and analysed at Shell UK Exploration and Production, London and K.S.E.P.L., Holland. The results indicate burial conditions similar to those estimated using illite crystallinity data, and confirm that apatite fission tracks were likely reset by post-depositional burial conditions, whereas zircon fission track data were unaffected.

Interpretations of fission track data

In view of the illite crystallinity, vitrinite reflectance and spore colour data, we consider that the zircon fission track ages represent the timing of cooling in the source region.

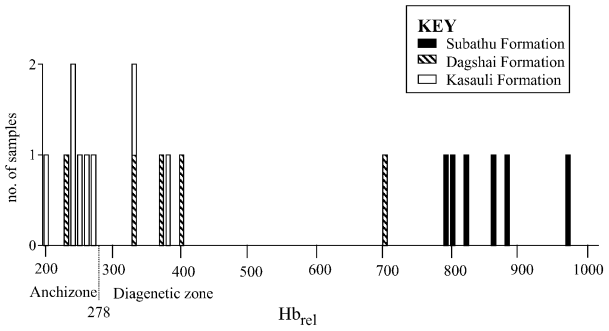

Fig. 4. Illite crystallinity values (Hb_{rel}) of the $< 2\,\mu m$ (diagenetic) component of foreland basin mudstone samples. Diagenetic-anchizone boundary after Blenkinsop (1988).

By contrast, apatite fission tracks ages represent the timing of cooling after burial in the basin.

Basin stratigraphy and provenance

Figure 3 shows that detrital zircons with a fission track age of 31 Ma were present in the basal Dagshai Formation sample Hm96-9A, a characteristic quartz-rich green sandstone found at the Subathu–Dagshai Formation contact, as described below. This age, interpreted as the time of cooling in the source region, provides a maximum age for the base of the Dagshai Formation at younger than 31 Ma. In view of the dating for the top of the underlying Subathu Formation succession at Early Lutetian at this locality

Table 2. Vitrinite reflectance values used to estimate maximum palaeotemperatures.

Sample number	Formation	Mean vitrinite reflectance	Maximum palaeotemperature (°C)
Hm91-10B	Dagshai–Kasauli transition*	1.60	195
Hm91-12B	Kasauli	1.13	159

*Informally termed the Kumahatti–Solon unit by Najman & Garzanti (2000), sedimentary rocks at this location resemble the Kasauli Formation sedimentologically, but resemble the Dagshai Formation petrographically.

Table 3. Spore colour fluorescence indices used to estimate maximum palaeotemperatures.

Sample number	Formation	Object	Fluorescence colour	Maturity estimation	Maximum palaeotemperature (°C)
Hm91-12B	Kasauli	algae	orange	0.95–1.10	140–156

Table 4. Facies Associations interpreted for the Dagshai, Kasauli and Dharamsala sediments.

Facies association	Summary description	Facies (see Table 5)	Interpretation	Relation between facies associations
CH	Multistorey sandstone unit, 2–12 m thick total (Subathu sub-basin) 5–60 m (Kangra sub-basin), erosively based, wedge-shaped and/or tabular beds, individually thin–thick bedded, can fine-upward and show evidence of waning flow	Ss, St, Sm, Sh, Sb, Sl, Sh, Sr	Channeled flow	Commonly erodes into and overlain by FF
CS	Sheet sandstones, thin–thick bedded, wedge-shaped or tabular, can fine or coarsen up, can show evidence of waning flow, accretion surfaces, beds occur singly or successively (up to 6 m thick). Kangra Basin: beds usually fine up and often occur as single units up to 4 m thick	Sr, Sm, St, Sl, Sx, Sb	Sheet floods from crevasse splays	Interbedded with FF
FF	Thin bedded interbedded fine-grained sandstone, siltstone and mudstone, thin to thick mudstone and siltstone and caliche. Can fine or coarsen up	Fl, Fsm, Fm, Fr, P	Floodplain overbank deposits	Commonly found interbedded with CS, can be cut down into and underlain by CH

CH, channeled; CS, crevasse splay; FF, floodplain fines.

(Batra, 1989), and early Eocene along strike (Blondeau *et al.*, 1986), this therefore conclusively proves the existence of a major unconformity, of more than 12 Myr duration. The Himalayan age of the zircon population confirms its source as the rising Himalayan thrust belt to the north. Pre-Himalayan aged populations found in some samples reflect erosion from source regions where Himalayan metamorphism did not exceed the temperature of the zircon PAZ, probably shallow levels of the thickened crust.

Propagation of thrusting into the foreland basin

Apatite fission track data were analysed from Kasauli Formation sample Hm96-25B collected from the hanging wall of the Bilaspur thrust (Fig. 2). This thrust delineates the northernmost extent of the Neogene Siwalik Group and separates imbricate thrusts and folds of the Palaeogene – E. Miocene Subathu, Dagshai and Kasauli Formations in the hanging wall from less deformed Neogene sediments in the footwall. Thus, according to the convention used in Nepal, it would be defined as the MBT, but in India it is considered by most workers as a Sub-Himalayan thrust (see above). Regardless of terminology, the Bilaspur Thrust represents the propagation of thrusting from the Lesser Himalaya into the basin.

The data from the Kasauli Formation sample show cooling through the PAZ for apatite at 5 Ma, which we interpret as cooling subsequent to maximum burial temperatures in the basin. The fission track length distribution suggests that cooling was rapid, best interpreted as due to rapid exhumation subsequent to thrusting along the Bilaspur Thrust. We therefore suggest that the movement of the Bilaspur Thrust occurred prior to 5 Ma, which indicates that thrusting had propagated from the Lesser Himalaya and into the foreland by this time.

FACIES OF THE EARLIEST CONTINENTAL FORELAND BASIN SEDIMENTS (TABLES 4 AND 5)

This paper primarily focuses on the initiation of continental sedimentation in the Himalayan foreland basin as documented by the Dagshai and Kasauli Formations and Dharamsala Group. The older marine sedimentary rocks of the Subathu Formation and younger alluvial Siwalik Group are described in detail elsewhere (e.g. Mathur, 1978, 1979; Meigs *et al.*, 1995; Burbank *et al.*, 1996 and references therein).

Subathu sub-basin

The Subathu–Dagshai Formation contact

As described above, the Subathu Formation facies consists of mudstones, sandstones and limestones deposited in a shallow marine environment. The Subathu–Dagshai Formation contact is relatively sharp and well defined, and there is no observable angular unconformity. The contact is marked by a varying combination of variegated shales, and characteristic green or quartz-rich sandstone, which Mathur (1977) termed the 'passage beds' (Fig. 5). At the contact localities near Dhondan (located in Najman *et al.*, 1993, their Fig. 4, also locatable on Fig. 2 where sample Hm96-9A was collected), the variegated shales show geochemical similarity to the Subathu Formation on account of their high Ni and Cr composition, characteristic of Subathu Formation mudstones and dissimilar to that found in

Table 5. Facies found in the Dagshai, Kasauli and Dharamsala facies associations of Table 4.

Facies code	Sediment type	Sedimentary structure
Ss	Very fine- to medium-grained sandstone. Can be pebbly	Scour surface. Can contain mud rip up clasts, plant material, flute and tool marks, cross-beds
St	Fine- and medium-grained sandstone. Can be pebbly	Trough cross-beds
Sp	Very fine- to medium-grained sandstone	Planar cross-beds
Sl	Very fine- to medium-grained sandstone	Low angle cross-beds
Sx	Very fine- to medium-grained sandstone	Cross-beds (undifferentiated)
Sh	Very fine- to medium-grained sandstone	Horizontal lamination
Sm	Very fine- to medium-grained sandstone	Massive (or faint lamination; Kangra Basin only)
Sr	Very fine- to medium-grained sandstone	Ripple marks
Sb	Fine- to medium-grained sandstone	Bioturbation
Fl	Subathu Basin: very thinly bedded, interbedded fine-grained sandstone, siltstone and mudstone. Kangra Basin: sandstone, siltstone, mudstone, finely laminated	Horizontal/undulose laminations, ripples
Fsm	Very thinly bedded, interbedded siltstone and mudstone	Horizontal/undulose laminations
Fm	Siltstone and mudstone	Massive
Fr	Siltstone and mudstone	Bioturbation
P	Caliche	Calcareous nodules
C	Coal, carbonaceous mud	Plant and mud films

Abbreviations adapted from Miall (1996).

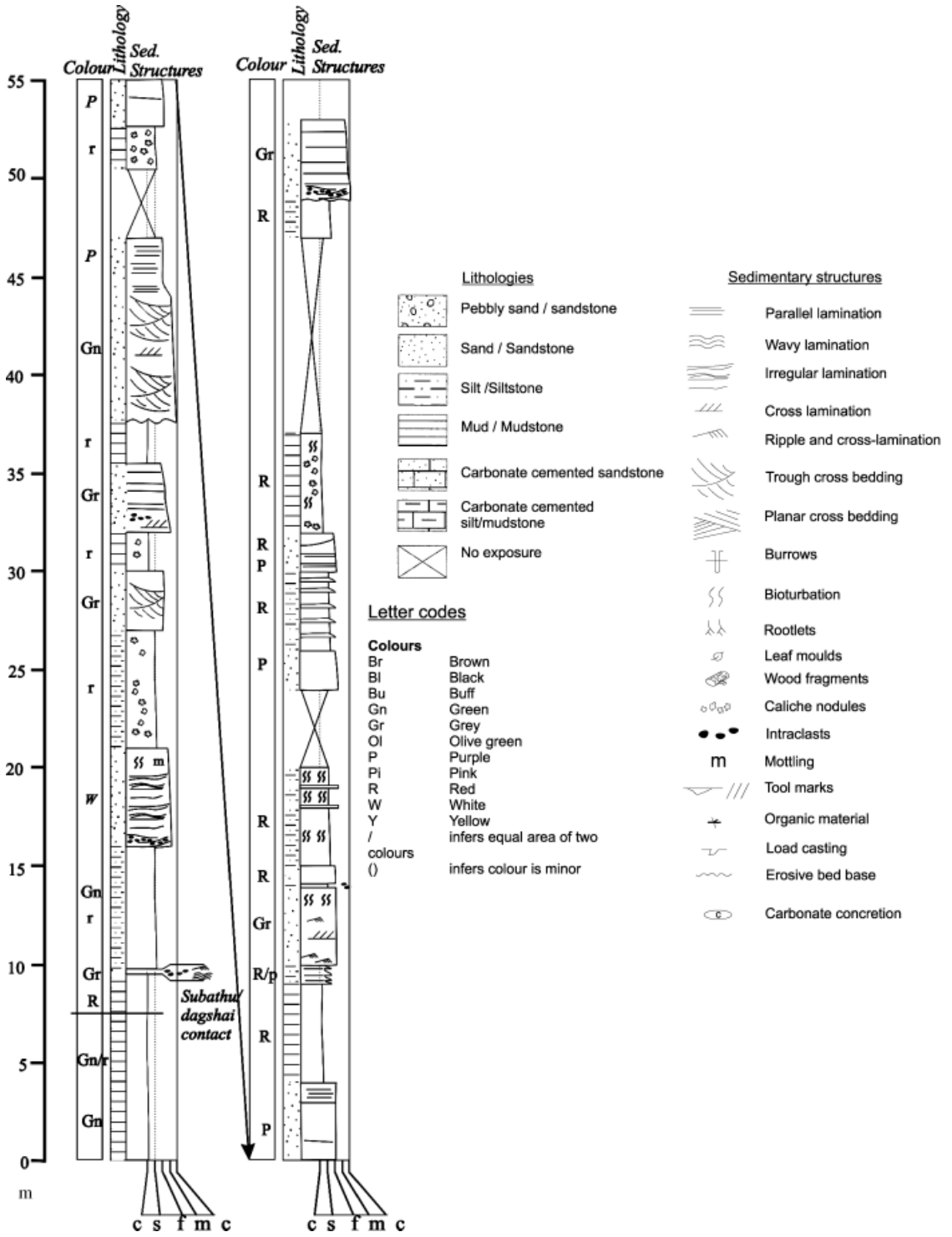

Fig. 5. Sedimentary log of the Subathu–Dagshai Formation contact. Log located in Fig. 2 (boxed no. 1), measured on the Bilaspur–Simla Highway, culvert 51/6, GPS co-ordinates: N31°15′00.0″ E076°54′48.1″.

Dagshai Formation mudstones (Najman & Garzanti, 2000). The variegated shales, which overlie classic Subathu Formation sediments, are red and green mottled. X-ray diffraction analysis shows the presence of quartz, illite, anatase and haematite. Up to 8 m, but usually less than 2 m of red sediment (mostly mudstones and siltstones which locally is burrowed, and rare fine sandstones with ripple marks and mud lenses) separates the top of the Subathu Formation from the overlying characteristic green or quartz-rich sandstone. This characteristic sandstone unit is assigned to the Dagshai Formation on account of its Sm–Nd geochemical signature, which is similar to that of the Dagshai Formation and dissimilar to that of the Subathu Formation (Najman *et al.*, 2001) and its position above classic Dagshai Formation facies red beds. This sandstone was deposited after 31 Ma as determined from a detrital zircon age obtained from sample Hm96-9A (this study). The sandstone occurs as either a single unit, 6–10 m thick,

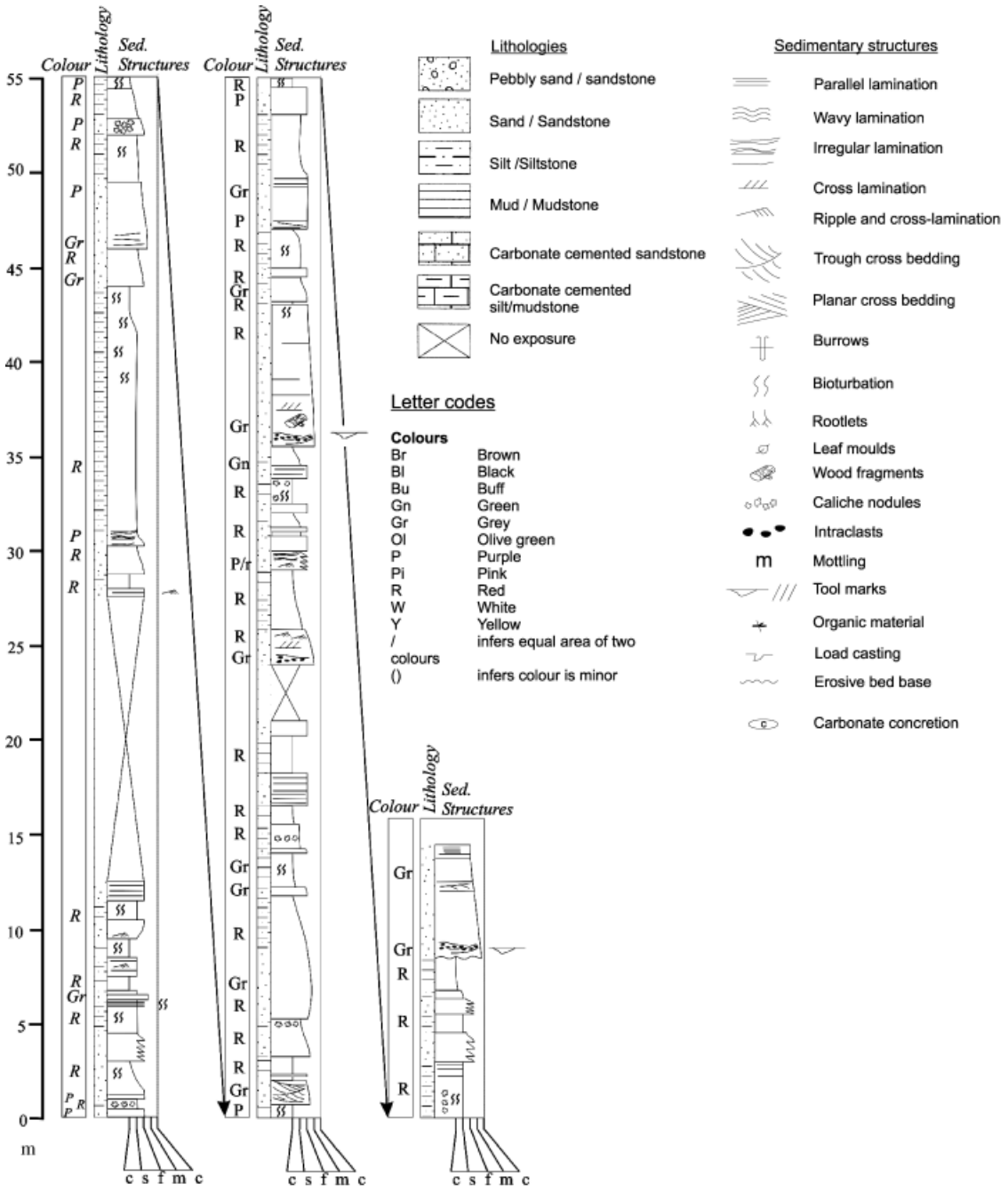

Fig. 6. Sedimentary log of Dagshai Formation, located in Fig. 2 (boxed no. 2). Log measured on the Kumahatti–Nahan Highway, culvert 16/4, GPS co-ordinates N30°49′16.1″E077°05′49.5″.

or as up to three units, 2.5–8 m thick, separated by up to 5 m of red sandstones, siltstones, mudstones and caliche. These green or quartz-rich sandstones are fine-medium grained, locally show fining-up, are thin- to thick-bedded, tabular and wedge-shaped and are erosively based on occasions with mud rip-up clasts. Sedimentary structures include parallel laminations, cross-beds and mottling due to bioturbation. Extremely rare palaeocurrent indicators (cross-beds, one locality, $n = 6$) show NE-directed flow. The basal Dagshai Formation sandstone beds are more winnowed, better sorted, have more well-rounded grains and are more quartz-rich than Dagshai Formation beds higher up in the succession.

The Dagshai Formation

The Dagshai Formation is characterised by its red colour, and consists of red mudstone and siltstone, caliche and red and grey sandstone (Fig. 6). The mudstones and siltstones are thin- to thick-bedded: the thin beds are commonly interbedded with very fine- to fine-grained, thin- to thick-bedded tabular sandstones, whereas the thick beds locally occur fining- and occasionally coarsening-up. Interspersed within these fine-grained facies are thin- to thick-bedded fine-grained sheet sandstones. Coarser-grained sandstone occurs in medium to thick beds, organised either singly or in multistorey units. These beds are

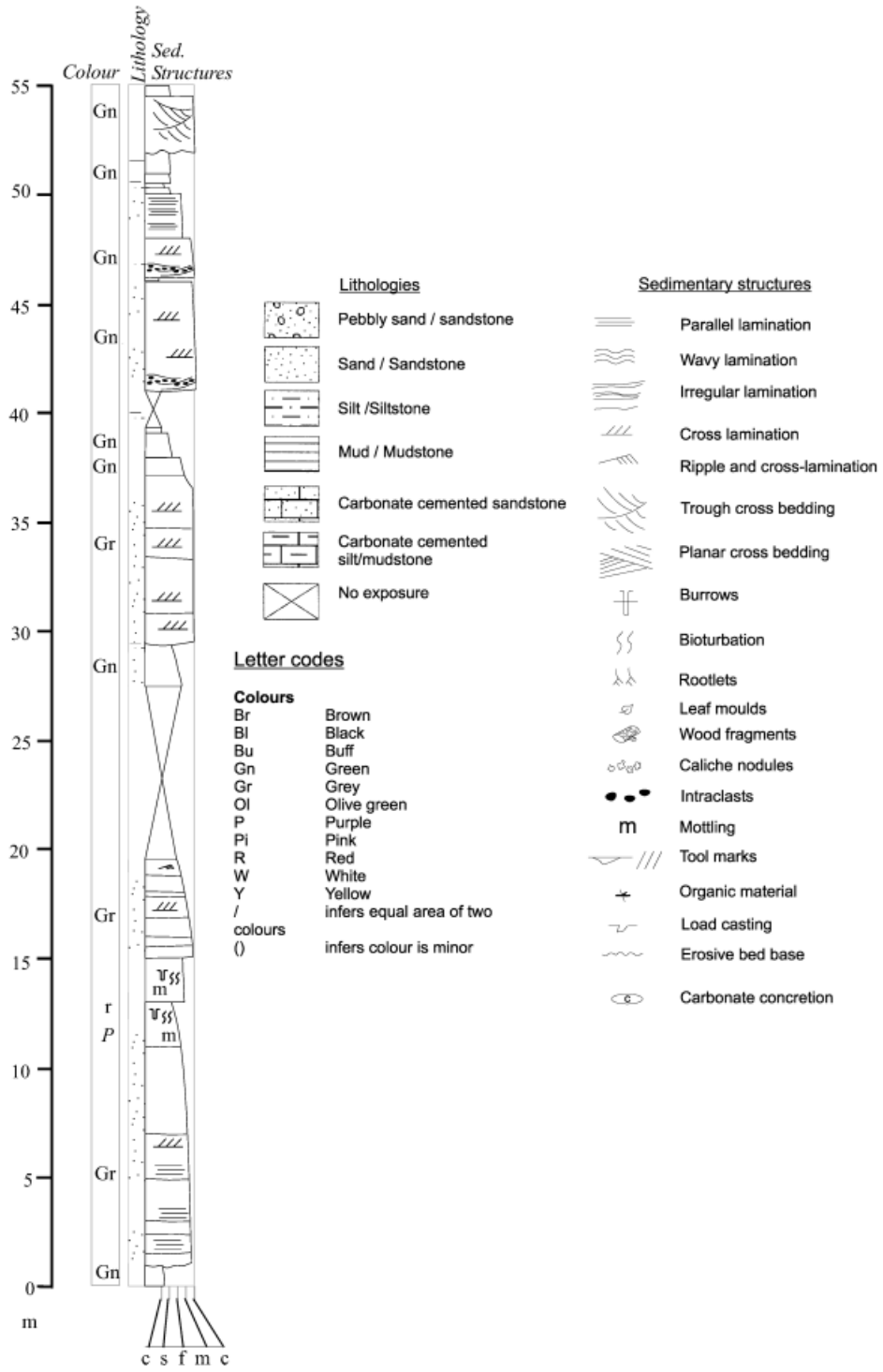

Fig. 7. Sedimentary log of the Kasauli Formation, located on Fig. 2 (boxed no. 3). Log measured on the Kumahatti–Nahan Highway, culvert 36/6, GPS co-ordinates: N30°42′59.2″ E077°11′26.1″.

tabular or wedge-shaped, locally have erosive bases with flute casts, gutter casts and mud rip-up clasts and locally show cross-bedding, ripple and horizontal lamination. Bioturbation is very common. Some beds fine upwards. Rarely, fossil logs are found at the base of sandstone beds.

Thick units of fine-grained facies and sheet sandstones constitute a significant part of the formation. Palaeocurrent indicators are relatively rare in this formation. Those present, taken from cross-bedding, ripples, flute marks and gutter casts at scattered locations ($n = 47$) indicate a NW and a SE–SW component of flow.

Kasauli Formation

The Kasauli Formation consists dominantly of grey-coloured multistoreyed sandstone beds separated by minor grey/green and occasionally red mudstone-siltstone units (Fig. 7). The mudstone–siltstone units are thin- to thick-

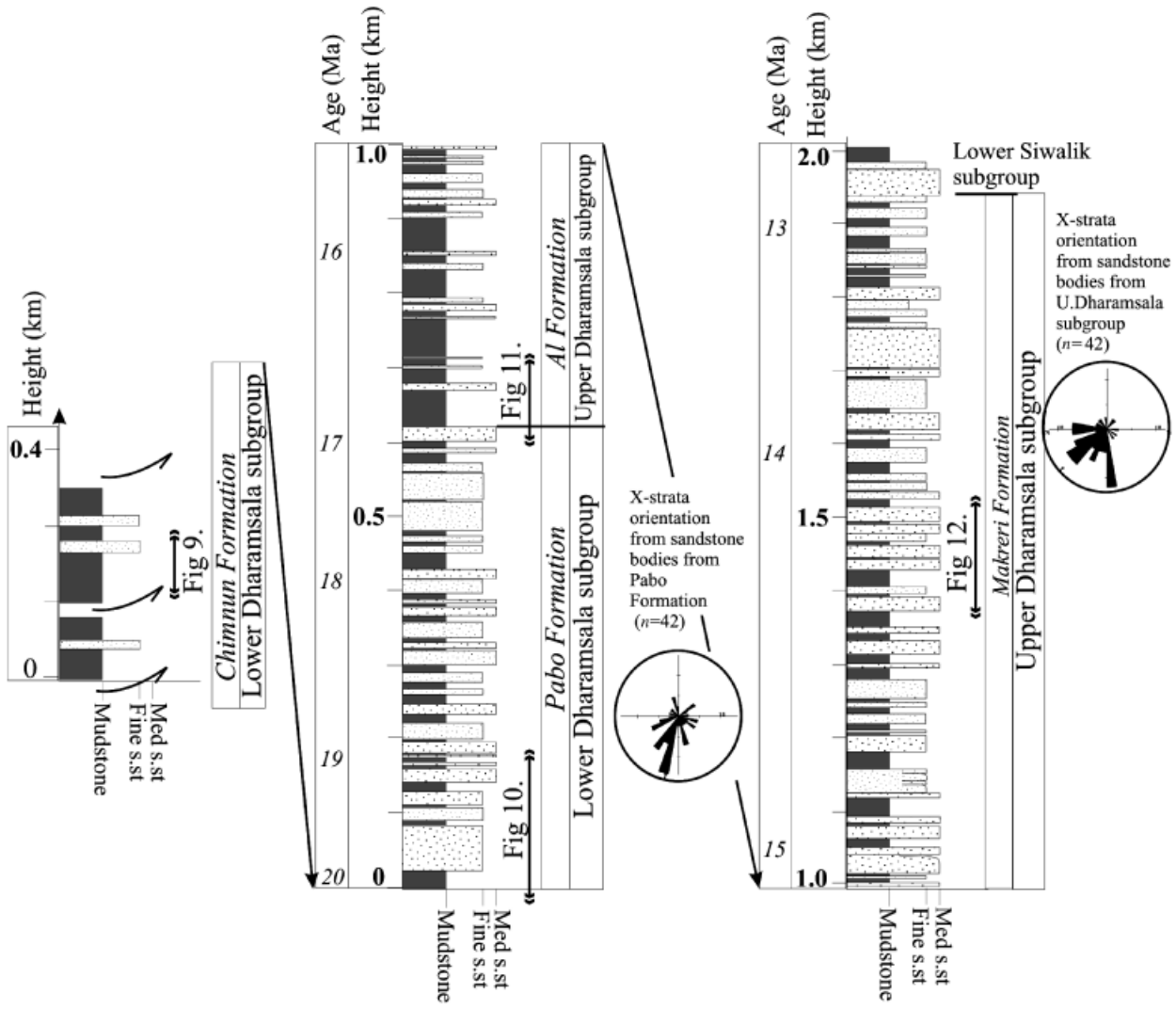

Fig. 8. Kangra Basin Dharamsala Group summary stratigraphy and palaeocurrent data collected from the Chimnun–Makreri–Birdhar road section (section located in Fig. 2). Magnetostratigraphic ages taken from White *et al*. (2001). Chimnun Formation succession is discontinuous and incomplete due to tectonic disruption by thrusting. The remainder of the succession is continuous and represents largely complete sections. Locations for detailed sedimentary logs are shown; Figs 9–12.

bedded, and locally contain well-preserved fossil leaves. Sandstone beds are medium- to thick-bedded, tabular or wedge shaped. They locally have erosive bases, with mud-rip up clasts and flute marks present on occasions. Logs, 1–5 m long, are commonly found at the base of sandstone beds. Cross-lamination, cross-bedding and bioturbation are found within some beds. The beds often fine-up.

In contrast to the Dagshai Formation, fine-grained facies only constitute a minor part of the sedimentary succession. Palaeocurrent indicators, more abundant than in the Dagshai Formation, and taken from gutter casts and flute marks at scattered locations ($n = 38$), again show palaeoflow to the NW and SE–SW.

Facies interpretation

The basal Dagshai Formation sandstone. The difference between the basal Dagshai Formation sandstone (the characteristic green/quartzitic sandstone) and the main Dagshai Formation has been previously explained by interpretation of the quartzitic sandstone as a beach sand (Singh & Khanna, 1980; Raiverman *et al*., 1983; Srivastava & Casshyap, 1983). However, typical beach sedimentary structures are rare and the sandstones are commonly erosively based. A coalesced mouth bar in a fluvial-dominated delta that experienced wave reworking, similar to the environment that produced the laterally extensive Lafourche lobe sandsheets of the Mississippi delta (Fisk, 1955), is another possibility, but evidence of marine influence or fauna is rare. Possible indistinct hummocky cross-stratification, indicative of shelf facies, is found at one locality, but the association with caliche is atypical. Rare flaser-bedding, most commonly associated with a tidal environment, also occurs, but in the absence of any associated sedimentary structures is weak evidence on which to base an interpretation.

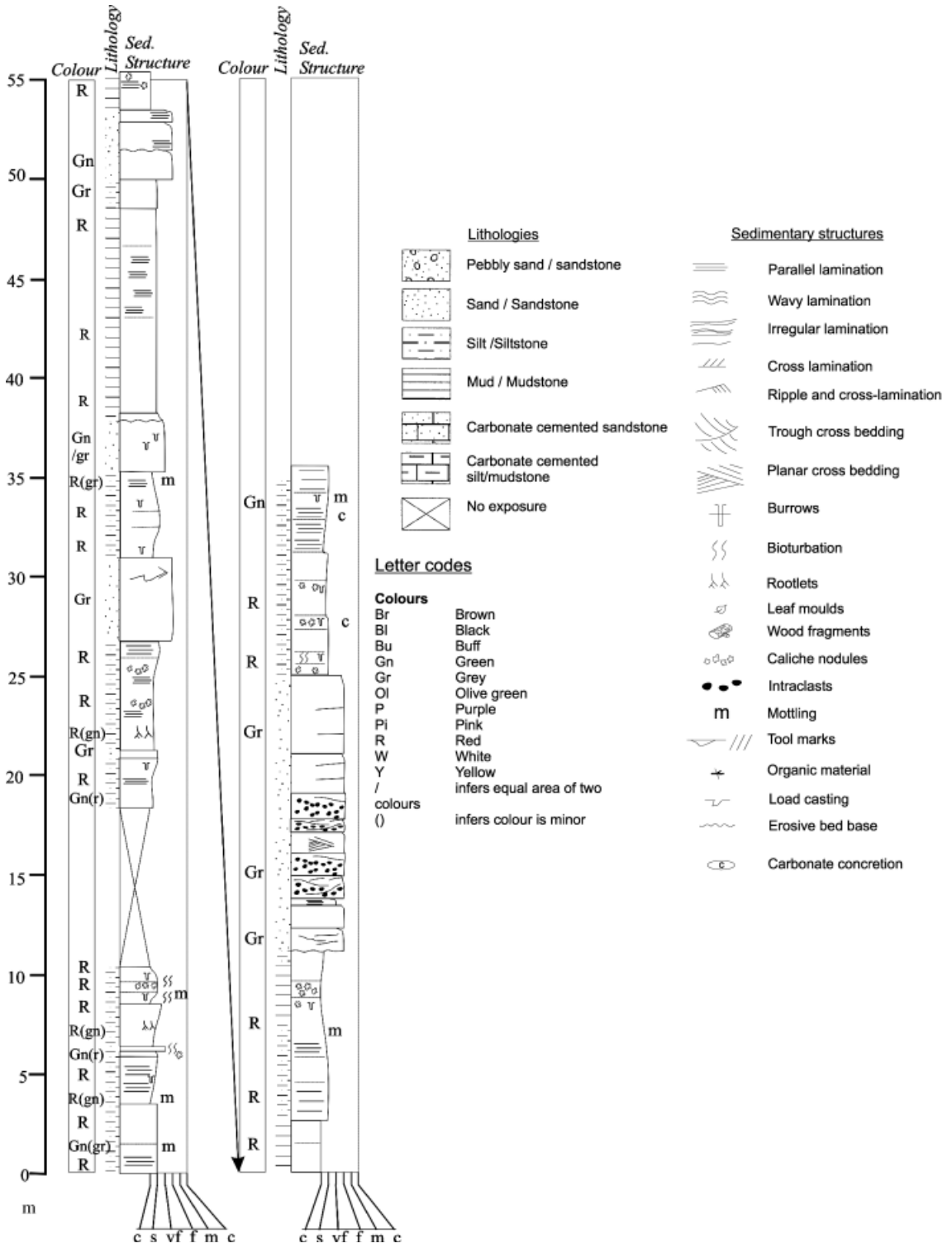

Fig. 9. Sedimentary log of the Chimnun Formation, Lower Dharamsala subgroup, Kangra sub-basin. Log location is on the Chimnun–Makreri–Birdhar road section, located in Figs 2 and 8.

Likewise, we consider dilution of the Himalayan source by a quartz-rich source from the Indian craton to the south, possibly an uplifted peripheral forebulge, to be an unlikely possibility. Sm–Nd and Rb–Sr whole rock isotopic signatures of the foreland basin sedimentary rocks record the predominance of a Greater Himalayan provenance from the base of the Dagshai to the present day (Najman *et al*., 2001) with little variation through time. This would argue against the substantial input of an Indian craton source at the base of the sequence.

Two likely facies interpretations for the quartzitic sandstone are:

(1) Extensive weathering during prolonged storage in alluvial plains, during which time tropical weathering

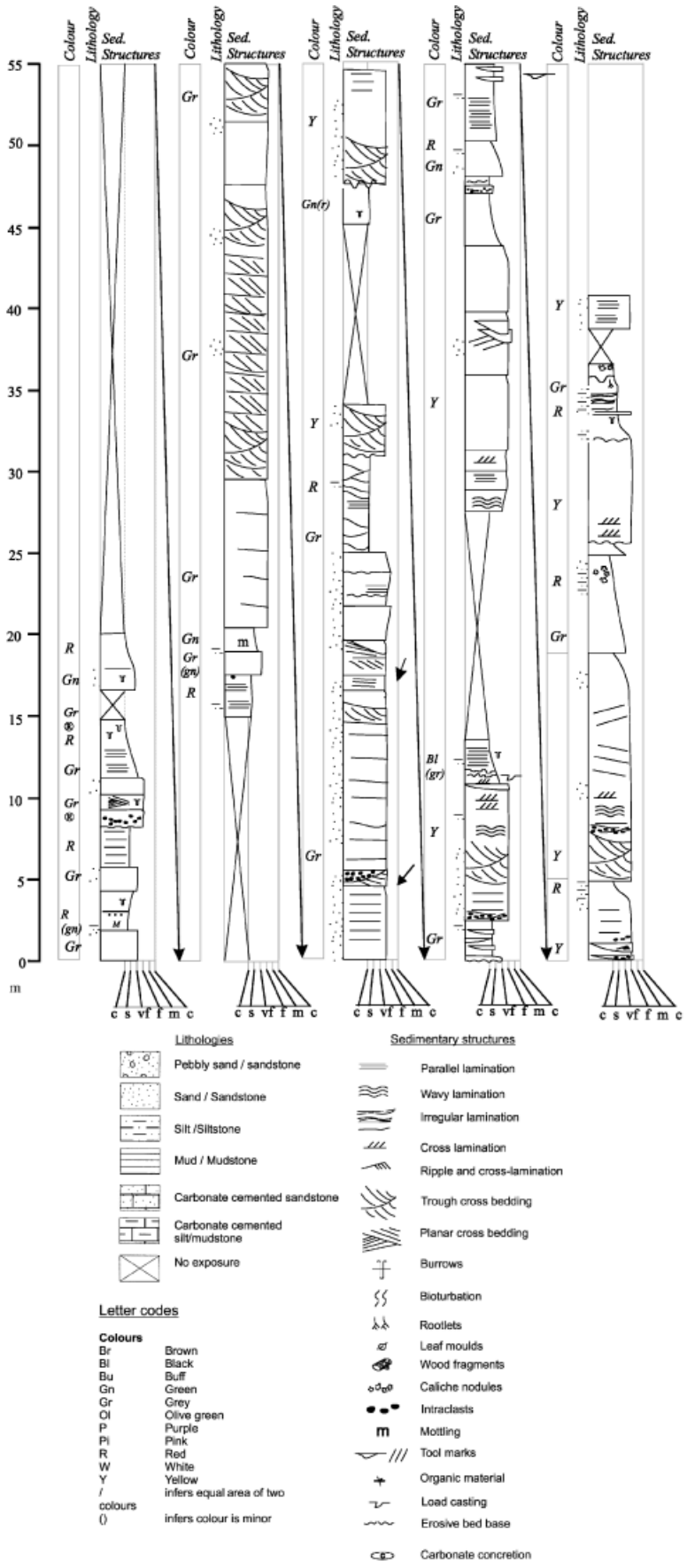

Fig. 10. Sedimentary log of the Pabo Formation, Lower Dharamsala subgroup, Kangra sub-basin. Log location is on the Chimnun–Makreri–Birdhar road section, located in Figs 2 and 8.

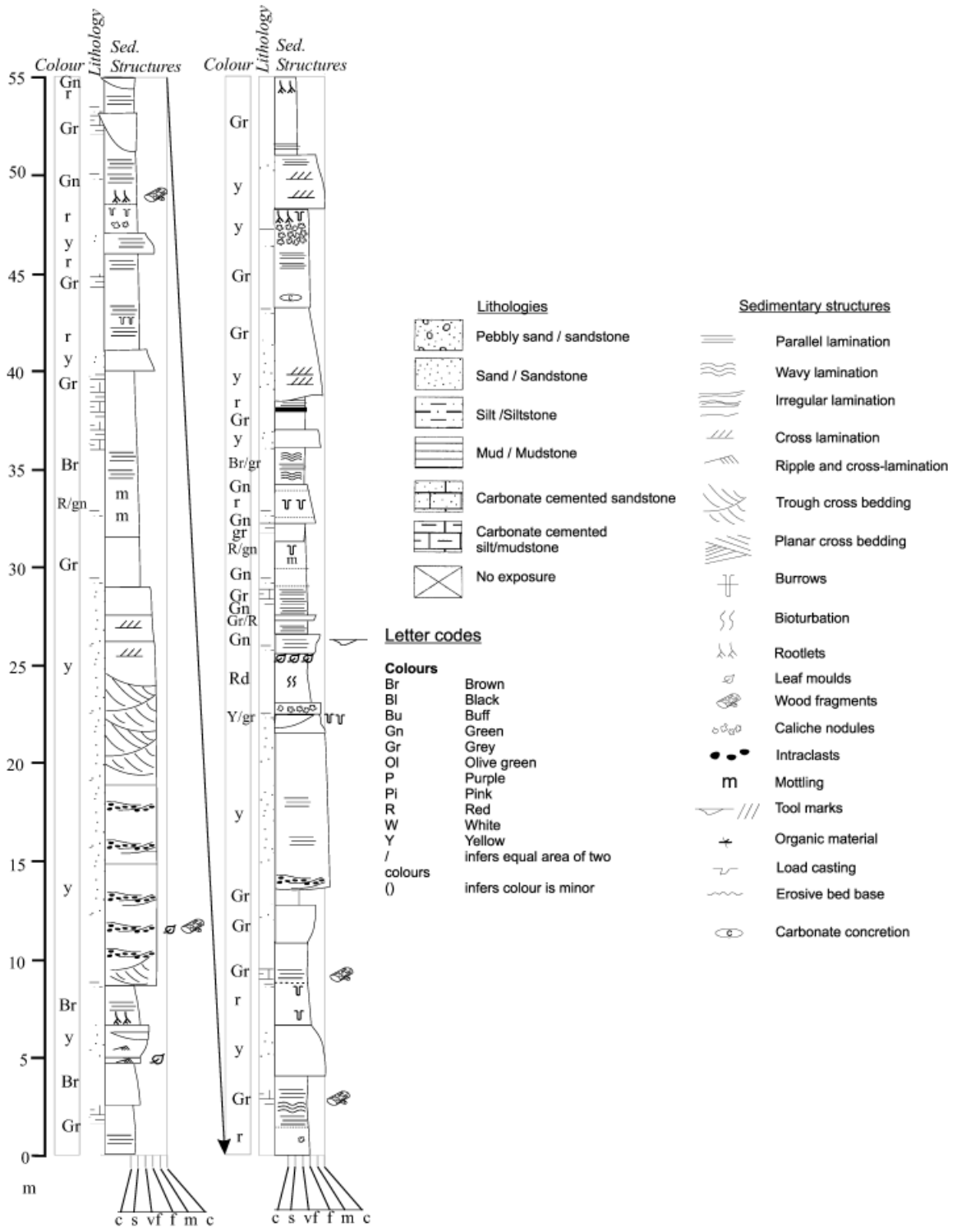

Fig. 11. Sedimentary log of the Al Formation, Upper Dharamsala subgroup, Kangra sub-basin. Log location is on the Chimnun–Makreri–Birdhar road section, shown in Figs 2 and 8.

and laterite formation caused the breakdown of labile elements and feldspar. This influence on alluvial sediments has been documented by Johnsson *et al.* (1988) for Andean foreland basin sediments subjected to intense tropical weathering. The position of the Himalayan foreland basin depositional site within a few degrees of the equator during the Eocene (Besse & Courtillot, 1988) makes this scenario likely, and the presence of distinctive haematite-cemented quartzarenite grains and ferricrete fragments within these beds supports this hypothesis (Najman & Garzanti, 2000).

(2) Recycling of quartzose Indian margin sandstones to the north in the earliest stages of collision.

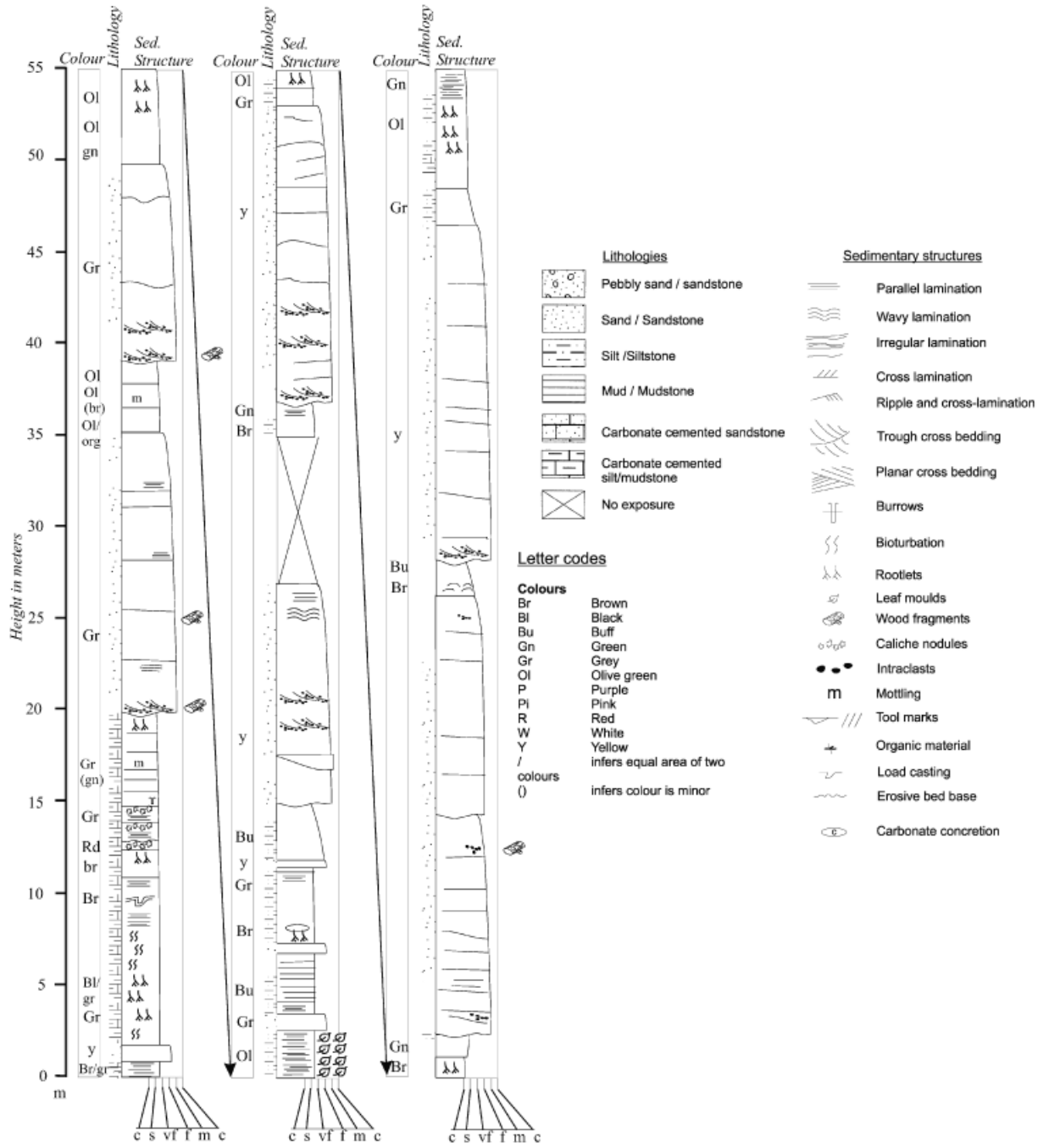

Fig. 12. Sedimentary log of the Makreri Formation, Upper Dharamsala subgroup. Log location is on the Chimnun–Makreri–Birdhar road section, shown in Figs 2 and 8.

Dagshai and Kasauli Formations. Previous interpretations of the depositional environment of the Dagshai Formation include deep-water turbidites (Chakraborty *et al*., 1962; Raman & Ravi, 1963; Raiverman & Seshavataram, 1965; Bhattacharya, 1970), a shallow epicontinental sea (Bhattacharya & Raiverman, 1973), a shallow brackish water or marine environment (Datta 1970; Wadia, 1975; Krishnan, 1982), a shallow fresh-water environment (Chaudhri, 1966) and a tidal-flat and coastal environment (Raiverman & Raman, 1971; Singh & Singh, 1995). The overlying Kasauli Formation has been interpreted as being deposited by turbidity currents (Raiverman & Seshavataram, 1965) in a coastal barrier and fluvio-deltaic environment (Singh & Khanna, 1980), in a shallow freshwater, fast subsiding basin (Chaudhri, 1971) or on alluvial plains with rapidly shifting shallow braided streams (Singh, 1978).

The red beds, caliche, leaf prints and channel-related facies described in this study indicate an alluvial environment, and we subdivide the facies into three Facies Associations; channeled (CH), crevasse splay (CS) and floodplain fines (FF) (Table 4). Erosively based sandstones (Facies Association CH), found in both the Dagshai and

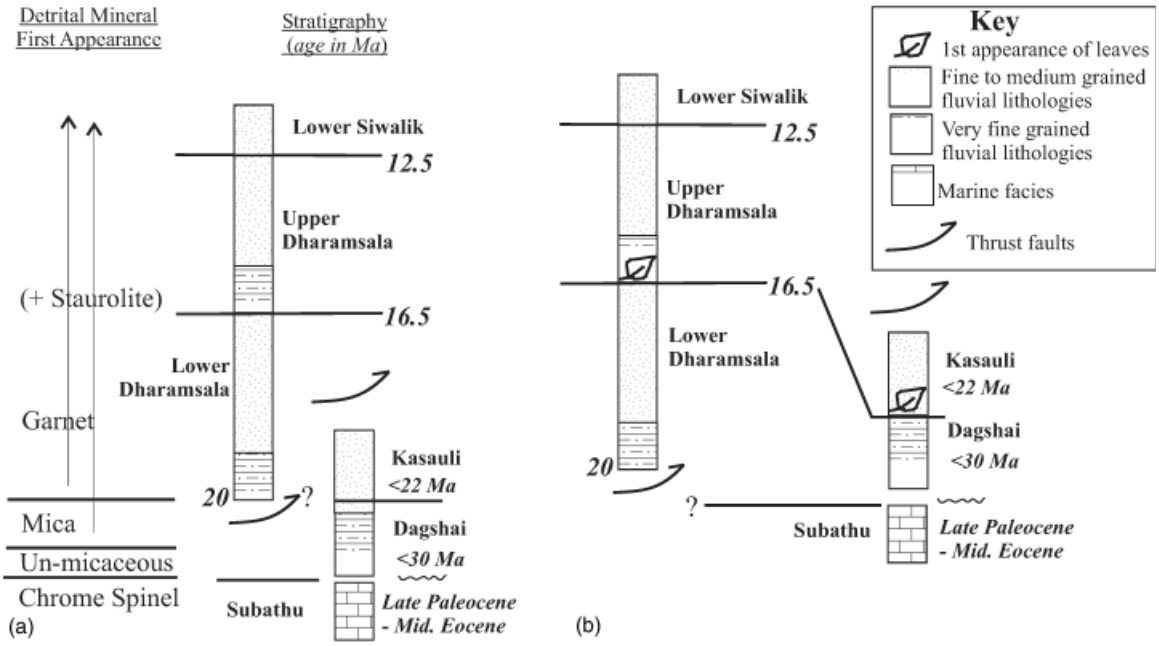

Fig. 13. Two alternative stratigraphic correlations between sediments of the Kangra and Subathu sub-basins in the foreland basin of northern India. (a) Erosional unroofing of the orogenic hinterland is taken as synchronous along strike in the orogen, (b) climatic change is taken as synchronous along strike in the orogen. For further discussion, see text.

Kasauli Formations, are interpreted as fluvial channels. Sheet flood deposits, consisting of thin- to thick-bedded tabular sandstones interbedded with floodplain fines are common in the Dagshai Formation and interpreted as the result of crevasse splay (Lithofacies Association CS). Facies Association FF, fine-grained mudstone/siltstone facies either thick-bedded and sometimes associated with caliche or thin-bedded and interbedded with thin-bedded fine-grained sandstones, represents overbank floodplain facies. CS Lithofacies Association is not recognised in the Kasauli Formation. FF lithofacies Association is rare in the Kasauli Formation and never includes caliche.

Whereas the Dagshai Formation consists of channel and tabular sandstones plus a significant proportion of fine-grained overbank floodplain facies, the Kasauli Formation consists predominantly of channelised sandstone beds. The Dagshai Formation, with its high proportion of fine-grained material would traditionally have been assigned a meandering fluvial facies (see review in Friend, 1983). However, preponderance of fine-grained facies is not unique to meandering fluvial facies. Material introduced to a floodplain by crevasse splay or flooding on fans may be unrelated to meandering facies and, although rare, braided river sediments may also consist of a significant proportion of overbank material (e.g. Rust, 1978; Bentham *et al*., 1993; Willis 1993a, b). We interpret the Dagshai Formation sediments as deposited where channels were present and the environment was conducive to overbank or sheet flooding and the build-up of thick floodplain deposits including caliche. By Kasauli Formation times, channel facies dominate. The sedimentary succession is typified by multistorey sandstone beds including beds that are erosionally based as well as those of tabular nonerosive form, and a lack of fine-grained facies. Kasauli formation rocks are interpreted as deposited in a braided fluvial regime where FF and CS Facies Associations are usually rare and shallow perennial sand-bed braided rivers are typified by channel-fill deposits consisting of simple tabular sheet sands (Miall, 1996).

The Kangra sub-basin

In contrast to the Subathu sub-basin where thrust truncations preclude logging of a continuous section through the sedimentary succession, the Kangra sub-basin has a near-continuous sedimentary sequence of the Dharamsala Group exposed (Fig. 8).

Chimnun Formation, Lower Dharamsala subgroup

The Chimnun Formation consists predominantly of massive or finely laminated, mottled, deep red and green micaceous mudstones and siltstones, which contain burrows, bioturbation, caliche nodules and rootlets (Fig. 9). These facies are interbedded with subordinate 1–2 m thick, grey, fining-up, massive, fine-grained, tabular sandstones, and rare grey, very fine- to fine-grained, lenticular or tabular, highly micaceous, flaggy (bedded on 10 cm scale), cross-stratified sandstone bodies 1–2 m thick. These bodies can be stacked into units up to 15–20 m in thickness. The formation contains three facies associations (Table 4) fine-grained facies (FF), which is dominant, interbedded with sheet sandstones (CS) and less common

channelised sandstones (CH). Palaeocurrent indicators are rare to absent.

Pabo Formation, Lower Dharmsala subgroup

The conformably overlying Pabo Formation (Fig. 10) comprises 5–20 m thick (and up to 60 m thick near the base of the Formation), laterally extensive, multistorey sandstone units, which fine upwards and grade into 1.5–10 m thick, finer-grained facies consisting of mudstones, siltstones and subordinate sandstones. The multistorey sandstone units have erosive lower contacts and comprise stacked sandstone bodies between 1 and 4 m thick, which are either massive and structureless or flaggy and cross-stratified. Although internal erosion surfaces are common within the multistorey unit, intraclast channel-lag deposits are rare.

The 1.5–10 m thick, finer-grained facies consist of grey, deep red or maroon mudstones, siltstones and sandy siltstones, interbedded with 0.5–3 m thick fine-grained to very fine-grained sandstone and siltstone. The mudstone–siltstone–sandy siltstone facies locally contain pedogenic carbonate nodules, occasional silcrete nodules, rootlets, burrows and mottling, often towards the top of the bed. The 0.5–3 m thick, fine-grained to very fine-grained sandstones and laminated siltstones usually occur as tabular sandsheets. The sandstone bases are usually nonerosive and flat, but occasionally small repeated chanellised units (20–50 cm thick) occur. The top of the bed usually grades up into the mudstones and siltstones with which it is interbedded. Beds may be massive or display cross-bedding, ripple cross-lamination or parallel lamination.

Facies associations are dominantly channel deposits (CH). Minor fine-grained facies (FF) are found between CH. Rare CS is interbedded with FF. The clearest palaeocurrent indicators are taken from mesoscale cross-strata from sandstone bodies within the multistorey units (CH) that, on the whole, show a dominant trend to the SSW (Fig. 8).

Al Formation, Upper Dharamsala subgroup

The Al Formation conformably overlies the Pabo Formation (Fig. 11). The proportion of sandstones to mudstones decreases, and channelised multistoreyed sandstones virtually disappear. There is an increase in carbonate cementation. Olive mudstones, which contain abundant leaf moulds and carbonaceous organic material, are common. Mudstones and siltstones of a variety of colours are interbedded with thin (ca. 0.5–2 m) sandstones sheets. Significant palaeocurrent indicators are rare to absent.

The facies associations of the Al Formation are dominated by fine-grained facies FF and interbedded sheet sandstones of CS. Channelised (CH) facies are a minor component.

Makreri Formation, Upper Dharamsala subgroup

The Makreri Formation sees a return to multistorey sandstone units (Fig. 12). These tabular, multistorey units are 8–30 m thick (up to 50 m towards the top of the succession) and laterally extensive for kilometres along strike. They typically comprise stacked, 1–3 m thick, massive, hard, grey, fine- to medium-grained sandstone beds. The sandstones are mostly structureless, although laminations and planar bedding are occasionally present. The multistorey bodies fine upwards. The contact between these sandstones and overlying mudstones and siltstones is gradational. Towards the top of the formation, at the base of the multistorey bodies, intraclasts of silt, mudstones, abundant woody fragments and fossil logs (0.5–2 m long, up to 0.5m wide) line erosive surfaces at the base of some of the sandstone beds or 'float' in the sandstone matrix. The multistorey sandstones are separated by 5–20 m thick predominantly mudstone, siltstone and sandy siltstone facies, interbedded with 0.5–2 m thick, tabular beds of fine to very fined grained sandstone or siltstone. The mudstones and siltstones vary in colour between grey, black, deep red, bright red, brown, green, olive green and pale green. Olive green mudstones are found in association with pristine leaf moulds and other woody plant material. The structure and pedogenesis varies from bed to bed. Primary sedimentary structures are lacking in massive units where bioturbation is pervasive. Beds sometimes have fine laminations, ripple and wavy laminations. Burrows are common, and caliche is very common.

The chanelised sandstones (CH) dominate the formation, and are interbedded with fine-grained facies FF. CS Sheet sandstones are minor. Palaeocurrent data are rare because, in contrast to the Pabo formation, the Makreri Formation has fewer micas and more calcite cementation, which obliterates sedimentary structures and thus the beds are massive. Rare cross-beds in the multistorey sandstone bodies show flow predominantly to the W, SW and S (Fig. 8). Orientation of large fossil logs that line the base of the channels shows a dominant strike of 130° ($n = 16$), which we interpret as perpendicular to the main flow direction, possibly deposited parallel to the lee-side of dunes/bars within the fluvial channel. The inferred flow direction is therefore towards the SW.

Facies interpretation of the Dharamsala Group

Previous interpretations of the depositional environment of the Dharamsala Group are the same as those interpreted for the Dagshai and Kasauli Formations, as described above. From the presence of red beds, caliche, leaf moulds, logs and channel-related facies described above, we interpret the Dharamsala Group sediments as fully continental, deposited in an alluvial environment.

The Chimnun and Al Formations are dominated by FF and CS Facies Associations, which we interpret as overbank sediments deposited on distal floodplains subjected to periodic inundation by crevasse splay and/or sheet flows.

The Pabo and Makreri Formations are dominated by channel facies CH, as typified by thick multistoreyed sandstones and only minor fine-grained facies. We interpret that these units were deposited by large rivers, with the paucity of fine-grained facies and the complex nature of the sandstones bodies indicative of a braided fluvial environment. In the Pabo Formation, tabular sandstones found in association with the channel units are interpreted as shallow perennial sand-bed braided units. This facies is not found in the Makreri Formation.

Contrary to the Subathu sub-basin, where relatively rare palaeocurrent indicators are only present in isolated and scattered outcrops, palaeocurrent data from the Dharamsala Group have been collected from a continuous sedimentary succession (Fig. 8) and are therefore of more use for constructing palaeo-drainage. Two drainage systems commonly occur synchronously in foreland basins; an axial fluvial system running parallel with the mountain belt and draining to remnant ocean basins, and a transverse system draining from the thrust belt or peripheral forebulge and often dispersing radially from fluvial megafans (e.g. Burbank & Beck, 1991; Miall, 1995). Modern-day drainage in the Himalaya involves both transverse drainage (e.g. Sutlej and Beas Rivers) and axial rivers (e.g. Ganges and Lower Indus rivers) draining to the Indus Fan in the west and the Bengal Fan in the east. Dumri Formation sediments in Nepal, co-eval with the Dharamsala Group, have palaeocurrent indicators documenting drainage towards the south to west–south-west, which DeCelles *et al.* (1998a) interpreted as axial drainage towards the west, i.e. opposite to the direction of axial drainage today in this region. Our data from the Dharamsala Group do not show any evidence for westerly draining axial drainage in the Kangra sub-basin during the Early–Mid-Miocene. These rocks were most likely deposited by transverse rivers.

Correlation of the pre-Siwalik sediments between the Subathu and Kangra sub-basins (Fig. 13)

Magnetostratigraphic dating of the Dagshai and Kasauli formation rocks is not possible due to structural complexity in the region, hence correlation with the Dharamsala Group can only be based on lithostratigraphy and maximum age constraints provided by detrital mineral dating. Below we outline two possible correlations, both of which are true to mineral age and magnetostratigraphic age constraints:

(1) Petrographic correlation: The Dagshai and Kasauli Formation sediments of the Subathu sub-basin record in their provenance a gradual unroofing of the metamorphosed Greater Himalaya, from very low to low-grade metamorphic detritus found in the Dagshai Formation, to low- to medium-grade metamorphic detritus found in the Kasauli Formation (Najman & Garzanti, 2000). The Lower Dharamsala subgroup has a close petrographic affinity with the Kasauli Formation, whereas the overlying Upper Dharamsala subgroup is unlike either the Dagshai or Kasauli Formations, and shows a predominance of detritus from sedimentary and low-grade metamorphic sources, the result of forward thrust propagation in the orogen (White *et al.*, 2002). These contrasting provenance histories may be a function of the individual tectonic histories within the catchment areas. The Subathu sub-basin most probably received sediments from the palaeo-Sutlej or palaeo-Yamuna rivers, whereas the Kangra basin received sediments draining from the palaeo-Beas. If we assume that the unroofing of the metamorphic core of the Greater Himalaya occurred synchronously, we interpret that the Dagshai Formation sediment, eroded from a very low to low-grade metamorphic source, was deposited prior to the Lower Dharamsala subgroup, eroded from a low- to medium-grade metamorphic source. As the base of the Lower Dharamsala subgroup is a faulted contact, it may be that an unexposed Dagshai-like equivalent was deposited below the Chimnun Formation in the Kangra basin. Using this petrographic correlation, we interpret that the Lower Dharamsala subgroup and Kasauli Formation were deposited contemporaneously. This was followed by a reversal of the unroofing trend due to the activation of a new thrust in the Kangra basin catchment, and deposition of the Upper Dharamsala subgroup.

(2) Climatic correlation: in this interpretation, the change from red bed and caliche facies, to facies with abundant logs, leaves and organic material, taken to represent the transition from an arid to a more humid environment, is used as the tie line. This change occurs between the Dagshai and Kasauli Formations in the Subathu sub-basin, and between the Pabo and Al Formations in the Kangra sub-basin. Using this correlation, the Dagshai Formation was deposited contemporaneously with the Lower Dharamsala subgroup, and the Kasauli Formation was deposited contemporaneously with the Upper Dharamsala subgroup. This would then suggest that erosional unroofing of the metamorphic core was diachronous along strike, with medium-grade metamorphic material appearing earlier in the Kangra basin than the Subathu Basin.

We prefer the second interpretation on the basis that climatic changes are more likely to occur synchronously basin wide compared with variations in erosional unroofing, and are therefore more likely to be a more robust time marker.

DISCUSSION

Combined with previously published data of the shallow marine facies of the Subathu Formation, we have shown that:

(1) Early evolution of the foreland basin involved sedimentation in a shallow marine environment followed by alluvial deposition.
(2) Marine and alluvial facies are separated by a major unconformity.
(3) Thrusting propagated into the foreland basin by 5 Ma.

Comparison with data along strike shows that these depositional patterns are characteristic of the foreland basin along its length. For example, in the Hazara–Kashmir syntaxis in Pakistan, shallow marine facies of the Patala Formation, dated at 53–55 Ma (Critelli & Garzanti, 1994), are overlain by continental facies of the Murree Formation dated at younger than 37 Ma (Najman *et al*., 2001), and similar patterns are recorded in the Kohat and Potwar plateaus (see Fig. 1). Likewise, in Nepal, Early–Mid-Eocene shallow marine facies of the Bhainskati Formation are unconformably overlain by Dumri alluvial sediments, with a distinctive oxisol at the contact.

DeCelles *et al*. (1998a) interpret the Bhainskati Formation as backbulge depozone deposits on the basis of their shallow facies and their Himalayan-derived provenance, similar to that of Subathu Formation in India (Najman & Garzanti, 2000). The Dumri Formation is interpreted as distal foredeep deposits, and the unconformity as a result of the cratonward migration of the forebulge through the backbulge depozone region. Redistribution of the load and slab break-off are also mechanisms that can cause the development of unconformities in distal foreland basin settings. Rejuvenation of the load in the internal parts of a thrust wedge by processes such as out-of-sequence thrusting, backthrusting or underplating can cause a forebulge to migrate towards the orogen causing unconformity in the distal region (Sinclair *et al*., 1991). Slab break-off is the gravity-driven detachment of subducted oceanic lithosphere from the light continental lithosphere that follows it into the subduction zone (von Blanckenburg & Davies, 1995; Davies & von Blanckenburg, 1995). This process results in a rapid isostatic uplift and can also cause redistribution of the load due to resultant backthrusting, both effects resulting in unconformity. Relaxation of a visco-elastic lithosphere and eustatic sea-level changes are also common processes by which unconformities may be developed in foreland basin settings, but we do not think them relevant to the Himalayan region. With stress relaxation, unconformities should develop during periods of tectonic quiescence (Quinlan & Beaumont, 1984; Beaumont *et al*., 1988), which is clearly not the case for the Himalaya where a variety of evidence indicates significant tectonism at this time (e.g. Prince *et al*., 1999; Vance & Harris, 1999; De Sigoyer *et al*., 2000). Sea-level changes are particularly important to development of unconformities on the distal cratonic side of the foreland basin (Posamentier & Allen, 1993), the likely location of the Subathu Formation. However, a number of large rapid sea-level changes occurred over the period of Subathu Formation deposition (Haq *et al*., 1987), which the Subathu Formation facies record, if at all, by a shallowing to brackish water only. It therefore seems unlikely that a sea-level fall of similar magnitude in the middle Eocene would result in $\sim$12 Myr hiatus, although global ice volume changes may have started to influence sedimentary successions by this time (Miller *et al*., 1987, 1991, 1996; Browning *et al*., 1996).

The lack of deep-water facies in the foreland basin is also intriguing. The classic peripheral foreland basin depositional model involves a progression from 'underfilled' (deep-water facies), through 'filled' (shallow marine and distal continental facies) to 'overfilled' (fully continental facies) stage, reflecting the changing balance between subsidence and sediment supply (*sensu* Covey, 1986; Allen *et al*., 1991; Sinclair & Allen, 1992). An interplay of a number of factors are modelled to control the development or otherwise of underfilled basin facies (e.g. Flemings & Jordan, 1989; Sinclair *et al*., 1991; Sinclair, 1997), including thrust front advance rates, rates of sediment supply and transport and crustal rigidity. The relatively rigid nature of the old, cold Indian crust has been cited as a possible cause for the lack of deep-water facies in the Himalaya (Garzanti *et al*., 1987), although there is substantial variation in rigidity today along strike, and the Indian crust loaded during the early stages of collision may have been weaker than that of today (Lyon-Caen & Molnar, 1985; Burbank *et al*., 1996). Potentially, flysch deposits and deep marine sediments may have been deposited further north in a more proximal position to the orogen and could be found either in the Tethys Himalaya or be concealed by overthrusting. Yet underthrusting of foreland basinal sediments is limited (e.g. Lyon-Caen & Molnar, 1985; Srivastava & Mitra, 1994; DeCelles *et al*., 2001), and no underfilled facies have yet been recorded in the Tethys Himalaya, although there is currently no data for the northern part of this region (Liu & Einsele, 1994).

Uplift and exhumation of the basin is constrained by the apatite fission track data, which indicates thrusting in the basin by 5 Ma. This is consistent with provenance and sedimentological facies data that show movement along the MBT, the thrust that separates the foreland basin from the Lesser Himalaya, by 11 Ma in the Kangra sub-basin (Meigs *et al*., 1995; Najman *et al*., 2002).

ACKNOWLEDGEMENTS

Andy Carter made significant contributions to the later stages of this manuscript; Peter Friend, Alastair Robertson, Hugh Sinclair and John Underhill contributed thought-provoking discussions on various topics discussed in this paper. Reviews by Peter DeCelles and Andrew Meigs considerably improved the manuscript. Ewan Laws, Andy Nayman and Douglas Paton provided excellent field assistance; Kuldeep Sharma and Das Raj are thanked for driving. This work was supported by a Royal Society Dorothy Hodgkin Fellowship and later a Royal Society International Fellowship awarded to the first author and an NERC studentship awarded to the third author. Cambridge University and Shell International Petroleum Co. Ltd provided additional fieldwork support.

REFERENCES

Allen, P.A., Crampton, S.L. & Sinclair, H.D. (1991) The inception and early evolution of the North Alpine Foreland Basin, Switzerland. *Basin Res.*, **3**, 143–163.

Aprahamian, J. & Paris, J.-L. (1981) Very low grade metamorphism with a reverse gradient induced by an overthrust in Haute-Savoie (France). In: *Thrust and Nappe Tectonics* (Ed. by K.P. McClay & N.J. Price), *Geol. Soc. London Spec. Publ.* **9**, 159–166.

Barker, C.E. & Pawlewicz, M.J. (1986) The correlation of vitrinite reflectance with maximum temperature in humic organic matter. In: *Paleogeothermics* (Ed. by G. Buntebarth & L. Stegena), pp. 79–93. Springer-Verlag, Berlin.

Batra, R.S. (1989) A reinterpretation of the geology and biostratigraphy of the Lower Tertiary Formations exposed along the Bilaspur–Shimla Highway, Himachal Pradesh, India. *J. Geol. Soc. India*, **33**, 503–523.

Beaumont, C. (1981) Foreland basins. *Geophys. J. Roy. Astronom. Soc.*, **65**, 291–329.

Beaumont, C., Quinlan, G. & amilton, J. (1988) Orogeny and stratigraphy: numerical models of the Palaeozoic in the eastern interior of north America. *Tectonics*, **7**, 389–416.

Bentham, P.A., Talling, P.J. & Burbank, D.W. (1993) Braided stream and flood-plain deposition in a rapidly aggrading basin: the Escanilla formation, Spanish Pyrenees. In: *Braided Rivers* (Ed. by J.L. Best & C.S. Bristow), *Geol. Soc. Spec. Publ.* **75**, 177–194.

Besse, J. & Courtillot, V. (1988) Palaeogeographic maps of the continents bordering the Indian Ocean since the Early Jurassic. *J. Geophys. Res.*, **93**, 11791–11808.

Bhatia, S.B. (1982) Facies, fauna and flora in the lower tertiary formations of northwestern Himalayas: a synthesis. *Palaeontol. Soc. India Spec. Publ.*, **1**, 8–20.

Bhatia, S.B. & Mathur, N.S. (1965) The occurrence of pulmonate gastropods in the Subathu–Dagshai passage beds near Dharampur, Simla Hills. *Bull. Geol. Soc. India*, **2**, 33–36.

Bhattacharya, N. (1970) Clay mineralogy and trace element geochemistry of Subathu, Dharamsala and Siwalik sediments in the Himalayan foothills of northwest India. *J. Geol. Soc. India*, **11**(4), 309–332.

Bhattacharya, N. & Raiverman, V. (1973) Clay mineral distribution of Dharamsala sediments in northwest India. *J. Geol. Soc. India*, **14**(1), 71–78.

Blenkinsop, T.G. (1988) Definition of low-grade metamorphic zones using illite crystallinity. *J. Metamorph. Petrol.*, **6**, 623–636.

Blondeau, A., Bassoullet, J.-P., Colchen, M., Han, T.L., Marcoux, J., Mascle, G. & Van Haver, T. (1986) Disparition des Formations Marines a L'Eocene Inferieur en Himalaya. *Sci Terre, Mem*, **47**, 103–111.

Browning, J.V., Miller, K.G. & Pak, D.K. (1996) Global implications of lower to middle Eocene sequence boundaries on the New Jersey coastal plain: the icehouse cometh. *Geology*, **24**, 639–642.

Burbank, D.W. & Beck, R.A. (1991) Models of aggradation versus progradation in the Himalayan foreland. *Geol. Rundsch.*, **80**/**3**, 623–638.

Burbank, D.W., Beck, R.A. & Mulder, T. (1996) The Himalayan foreland basin. In: *The Tectonic Evolution of Asia* (Ed. by A. Yin & T.M. Harrison), pp. 149–188. Cambridge University Press, Cambridge.

Chakraborty, A., Venkataraman, S. & Kumar, S.P. (1962) Report on the Geology of Parautochthon Belt in Hatkot–Kasauli–Subathu area in Mahasu district, H.P. and Patiala and Ambala districts, Punjab, Field Season 1961–62. Reports of the Oil and Natural Gas Commission, unpublished.

Chaudhri, R.S. (1966) Geology of the lower tertiary rocks of the Simla hills. Unpublished PhD Thesis, Punjab University, Chandigarh.

Chaudhri, R.S. (1971) Petrology of the Lower Tertiary formations of Northwestern Himalayas. *Bull. Indian Geol. Assoc.*, **4**, 45–53.

Coulon, C., Maluski, H., Bollinger, C. & Wang, S. (1986) Mesozoic and Cenozoic volcanic rocks from central and southern Tibet; ^{39}Ar–^{40}Ar dating, petrological characteristics and geodynamic significance. *Earth Planet. Sci. Lett.*, **79**, 281–302.

Covey, M. (1986) The evolution of foreland basins to steady-state: evidence from the western Taiwan foreland basin. In: *Foreland Basins* (Ed. by P.A. Allen & P. Homewood), *Spec. Publ. Int. Assoc. Sedimentol.* **8**, 7–90.

Crampton, S.L. & Allen, P.A. (1995) Recognition of forebulge unconformities associated with early stage foreland basin development: example from the North Alpine Foreland Basin. *Am. Assoc. Petrol. Geol. Bull.*, **79**, 1495–1514.

Critelli, S. & Garzanti, E. (1994) Provenance of the Lower Tertiary Murree redbeds (Hazara-Kashmir Syntaxis, Pakistan) and initial rising of the Himalayas. *Sediment. Geol.*, **89**, 265–284.

Datta, A.K. (1970) Some observations on the sedimentological and palaeontological aspects of the Subathu and Lower Dharamsala sediments in the Simla Hills area and their bearing on the tectonic evolution of the foothill belt. *Publ. Centre Adv. Study Geol., Punjab Univ., Chandigargh*, **7**, 23–30.

Davies, J.H. & von Blanckenburg, F. (1995) Slab breakoff: a model of lithospheric detachment and it's test in the magmatism and deformation of collisional orogens. *Earth Planet. Sci. Lett.*, **129**, 85–102.

DeCelles, P.G. & Giles, K.A. (1996) Foreland basin systems. *Basin Res.*, **8**, 105–123.

DeCelles, P.G., Gehrels, G.E., Quade, J. & Ojha, T.P. (1998a) Eocene-early Miocene foreland basin development and the history of Himalayan thrusting, western and central Nepal. *Tectonics*, **17**, 741–765.

DeCelles, P.G., Gehrels, G.E., Quade, J., Ojha, T.P., Kapp, P.A. & Upreti, B.N. (1998b) Neogene foreland basin deposits, erosional unroofing and the kinematic history of the Himalayan fold-thrust belt, western Nepal. *Geol. Soc. Am. Bull.*, **110**, 2–21.

DeCelles, P.G., Robinson, D.M., Quade, J., Ojha, T.P., Garzione, C.N., Copeland, P. & Upreti, B.N. (2001) Stratigraphy, structure and tectonic evolution of the Himalayan Fold-Thrust belt in western Nepal. *Tectonics*, **20**, 487–509.

De Sigoyer, J., Chavagnac, V., Blichert-Toft, J., Villa, I., Luais, B., Guillot, S., Cosca, M. & Mascle, G. (2000) Dating the Indian continental subduction and collisional thickening in the northwest Himalaya: multichronology of the Tso Morari eclogites. *Geology*, **28**, 487–490.

Fisk, H.N. (1955) Sand facies of recent Mississippi delta deposits. World Petrology Congress, Rome, pp. 377–398.

Flemmings, P.B. & Jordan, T.E. (1989) A synthetic stratigraphic model of foreland basin development. *J. Geophys. Res.*, **94**, 3851–3866.

Friend, P.F. (1983) Towards the field classification of alluvial architecture or sequence. In: *Modern and Ancient Fluvial systems* (Ed. by J.D. Collinson & J. Lewis), *Spec. Publ. Int. Assoc. Sedimentol.* **6**, 345–354.

Fuchs, G. (1982) The geology of western Zanskar. *Jahrb. Geol. Bundesanst.*, **125**, 513–540.

Gaetani, M. & Garzanti, E. (1991) Multicyclic history of the Northern India Continental margin (northwestern Himalaya). *Am. Assoc. Petrol. Geol. Bull.*, **75**, 1427–1446.

Galbraith, R.F. (1988) Graphical display of estimates having different standard errors. *Technometrics*, **30**, 271–281.

Galbraith, R.F. (1990) The radial plot: graphical assessment of spread in ages. *Nucl. Tracks Radiat. Meas.*, **17**, 207–214.

Gansser, A. (1964) *Geology of the Himalayas*. Interscience Publishers, London, 273pp.

Garzanti, E., Baud, A. & Mascle, G. (1987) Sedimentary record of the northward flight of India and its collision with Eurasia (Ladakh Himalaya, India). *Geodin. Acta*, **1**(4/5), 297–312.

Garzanti, E. & Van Haver, T. (1988) The Indus clastics: forearc basin sedimentation in the Ladakh Himalaya (India). *Sediment. Geol.*, **59**, 237–249.

Haq, B.U., Hardenbol, J. & Vail, P.R. (1987) Chronology of fluctuating sea levels since the Triassic (250 million years ago to present). *Science*, **235**, 1156–1167.

Harrison, T.M., Copeland, P., Hall, S.A., Quade, J., Burner, S., Ojha, T.P. & Kidd, W.S.F. (1993) Isotopic preservation of Himalayan/Tibetan uplift, denudation and climatic histories of two molasse deposits. *J. Geol.*, **101**, 157–175.

Hodges, K.V., Hubbard, M.S. & Silverberg, D.S. (1988) Metamorphic constraints on the thermal evolution of the central Himalayan Orogen. *Philos. Trans. R. Soc. London*, **326**, 257–280.

Honegger, K., Dietrich, V., Frank, W., Gansser, A., Thoni, M. & Trommsdorf, V. (1982) Magmatism and metamorphism in the Ladakh Himalaya (the Indus Tsangpo Suture Zone). *Earth Planet. Sci. Lett.*, **60**, 253–292.

Hurford, A.J. (1990) Standardization of fission track dating calibration: recommendation by the fission Track Working Group of the IUGS subcommission on geochronology. *Chem. Geol.*, **80**, 177–178.

Johnsson, M.J., Stallard, R.F. & Meade, R.H. (1988) First-cycle quartz arenites in the Orinoco River Basin, Venezuela and Columbia. *J. Geol.*, **96**, 263–277.

Johnson, N.M., Stix, J., Tauxe, L., Cerveny, P.F. & Tahirkheli, R.A.K. (1985) Palaeomagnetic chronology, fluvial processes and tectonic implications of the Siwalik deposits near Chinji Village, Pakistan. *J. Geol.*, **93**, 27–40.

Jordan, T.E. (1981) Thrust loads and foreland basin evolution, cretaceous, Western United States. *Am. Assoc. Petrol. Geol. Bull.*, **65**(12), 2506–2520.

Karunakaran, C. & Ranga Rao, A. (1979) Status of exploration for hydrocarbons in the Himalayan region – contributions to stratigraphy and structure. Oil and Natural Gas Commission, pp. 1–66.

Kisch, H.J. (1980a) Incipient metamorphism of Cambro–Silurian clastic rocks from the Jamtland Supergroup, central Scandinavian Caledonides: illite crystallinity and 'vitrinite' reflectance. *J. Geol. Soc. London*, **137**, 271–278.

Kisch, H.J. (1980b) Illite crystallinity and coal rank associated with lower grade metamorphism of the Taveyanne greywacke in the Helvetic zone of the Swiss Alps. *Ecologae Geol. Helv.*, **73**, 753–777.

Krishnan, M.S. (1982) *Geology of India and Burma*, 6th edn. CBS Publishers and Distributors, Delhi, India, 536pp.

Kubler, B. (1967) La crystallinite de l'illite et les zones tout a fait superieurs du metamorphisme: Colloque sur les 'Etages tectoniques'. Neuchatel, Festschrift, pp. 105–122.

Laslett, G.M., Green, P.F., Duddy, I.R. & Gleadow, A.J.W. (1987) Thermal annealing of fission tracks in apatite, 2, A quantitative description. *Chem. Geol.*, **65**, 1013.

Le Fort, P. (1996) Evolution of the Himalaya. In: *The Tectonic Evolution of Asia* (Ed. by A. Yin & T.M. Harrison), pp. 95–109. Cambridge University Press, Cambridge.

Le Fort, P., Cuney, M., Deniel, C., France-Lanord, C., Sheppard, S.M.F., Upreti, B.N. & Vidal, P. (1987) Crustal generation of the Himalayan leucogranites. *Tectonophysics*, **134**, 39–57.

Liu, G. & Einsele, G. (1994) Sedimentary history of the Tethyan basin in the Tibetan Himalayas. *Geol. Rundsch.*, **83**, 32–61.

Loyal, R.S. (1990) Lithostratigraphy of the basal Subathu Formation (Upper Palaeocene–Mid Eocene) exposed in the stratotype, Kuthar River, Subathu, Himachal Pradesh, India, with introductory notes on physiography and tectonics. *Tertiary Res.*, **12**, 1–16.

Lyon-Caen, H. & Molnar, P. (1985) Gravity anomalies, flexure of the Indian plate, and the structure, support and evolution of the Himalaya and Ganga Basin. *Tectonics*, **4**, 513–538.

Mathur, N.S. (1977) Age of the Tal and Subathu formations in the Garhwal region, Uttar Pradesh, India. *Bull. Indian Geol. Assoc.*, **10**(2), 21–27.

Mathur, N.S. (1978) Biostratigraphical aspects of the Subathu Formation, Kumaun Himalaya. *Recent Res. Geol.*, **5**, 96–112.

Mathur, N.S. (1979) Palaeoecology of the Subathu Formation, Kumaun Himalaya. *Bull. Indian Geol. Soc.*, **12**, 81–90.

Meigs, A.J., Burbank, D.W. & Beck, R.A. (1995) Middle–late Miocene (> 10 Ma) formation of the Main Boundary thrust in the western Himalaya. *Geology*, **23**, 423–426.

Metcalfe, R.P. (1993) Pressure, temperature and time constraints on metamorphism across the Main Central Thrust zone and High Himalayan Slab in the Garhwal Himalaya. In: *Himalayan Tectonics* (Ed. by P.J. Treloar & M.P. Searle), *Geol. Soc. Spec. Publ.* **74**, 485–510.

Miall, A.D. (1995) Collision-related foreland basins. In: *Tectonics of Sedimentary Basins* (Ed. by C.J. Busby & R.V. Ingersoll) Blackwell Science, Oxford, 579pp.

Miall, A.D. (1996) *The Geology of Fluvial Deposits*. Springer-Verlag, Berlin, 582pp.

Miller, K.G., Fairbanks, R.G. & Mountain, G.S. (1987) Tertiary oxygen isotope synthesis, sea level history and continental margin erosion. *Paleoceanography*, **2**, 1–19.

Miller, K.G. & Mountain, G.S.ODP Leg 150 Shipboard Party, and Members of the New Jersey Coastal Plain Drilling Project (1996) Drilling and dating New Jersey Oligocene–Miocene sequences: ice volume, global sea level, and Exxon records. *Science*, **271**, 1092–1095.

Miller, K.G., Wright, J.D. & Fairbanks, R.G. (1991) Unlocking the icehouse: Oligocene–Miocene oxygen isotopes, eustacy and margin erosion. *J. Geophys. Res.*, **96**, 6829–6848.

Najman, Y., Clift, P., Johnson, M.R.W. & Robertson, A.H.F. (1993) Early stages of foreland basin evolution in the Lesser Himalaya, N. India. In: *Himalayan Tectonics* (Ed. by P.J. Treloar & M.P. Searle), Geol. Soc. Spec. Publ. **74**, 541–55.

Najman, Y. & Garzanti, E. (2000) Reconstructing early Himalayan tectonic evolution and paleogeography from Tertiary foreland basin sedimentary rocks, northern India. *Geol. Soc. Am. Bull.*, **112**, 435–449.

Najman, Y., Garzanti, E., Pringle, M., Bickle, M., Burbank, D., Ando, S. & Brozovic, N. (2002) Exhumation and attainment of steady state in the Himalaya: insights from the

detrital sediment record. *Eos. Trans. AGU*, **83**, (47), T71A–1158 (Fall Meet. Suppl. Abstract)

Najman, Y., Pringle, M., Godin, L. & Oliver, G. (2001) Dating of the oldest continental sediments from the Himalayan foreland basin. *Nature*, **410**, 194–197.

Najman, Y.M.R., Pringle, M.S., Johnson, M.R.W., Robertson, A.H.F. & Wijbrans, J.R. (1997) Laser $^{40}Ar/^{39}Ar$ dating of single detrital muscovite grains from early foreland basin sediments in India: implications for early Himalayan evolution. *Geology*, **25**, 535–538.

Parkash, B., Sharma, R.P. & Roy, A.K. (1980) The Siwalik Group (molasse) – sediments shed by collision of continental plates. *Sediment. Geol.*, **25**, 127–159.

Parrish, R.R. & Hodges, K.V. (1996) Isotopic constraints on the age and provenance of the Lesser and Greater Himalayan Sequences, Nepalese Himalaya. *Geol. Soc. Am. Bull.*, **108**, 904–911.

Pearson, D.A. (1984) Approaching a pollen/spore colour standard. *Palynology*, **6**, 289.

Posamentier, H.W. & Allen, G.P. (1993) Siliciclastic sequence stratigraphic patterns in foreland ramp-type basins. *Geology*, **21**, 455–458.

Powers, P.M., Lillie, R.J. & Yeats, R.S. (1998) Structure and shortening of the Kangra and Dehra Dun reentrants, Sub-Himalaya, India. *Geol. Soc. Am. Bull.*, **110**, 1010–1027.

Prince, C.I., Foster, G., Vance, D., Harris, N. & Baker, J. (1999) The thermochronology of the High Himalayan Crystallines in the Garhwal Himalaya; Prograde history of a polymetamorphic slab. *Terra Nostra*, **99**, 119–120.

Quinlan, G. & Beaumont, C. (1984) Appalachian thrusting, lithospheric flexure and Paleozoic stratigraphy of the Eastern Interior of North America. *Can. J. Earth Sci.*, **21**, 973–996.

Raiverman, V., Kunte, S.V. & Mukherjea, A. (1983) Basin geometry, cenozoic sedimentation and hydrocarbon prospects in North Western Himalaya and Indo-Gangetic plains. *Petrol. Asia J.*, **6**, 67–92.

Raiverman, V. & Raman, K.S. (1971) Facies in the Subathu sediments, Simla Hills. Northwestern Himalaya, India. *Geol. Mag.*, **108**, 329–341.

Raiverman, V. & Seshavataram, B.T.V. (1965) On mode of deposition of Subathu and Dharmsala sediments in the Himalayan foothills in Punjab and Himachal Pradesh. Min. Metall. Soc. India, *Wadia Commemorative Volume*, 556–571.

Reuber, I. (1989) The Dras arc: two successive volcanic events on eroded oceanic crust. *Tectonophysics*, **161**, 93–106.

Reuber, I., Colchen, M. & Mevel, C. (1987) The geodynamic evolution of the south Tethyan margin in Zanskar, NW Himalaya, as revealed by the Spontang ophiolite melanges. *Geodin. Acta*, **1**, 283–296.

Robertson, A.H.F. & Degnan, P.J. (1993) Sedimentology and tectonic implications of the Lamayuru Complex: deep water facies of the Indian Passive margin. In: *Himalayan Tectonics* (Ed. by P.J. Treloar & M.P. Searle), *Geol. Soc. London Spec. Publ.* **74**, 299–322.

Rowley, D.B. (1996) Age of initiation of collision between India and Asia: a review of stratigraphic data. *Earth Planet. Sci. Lett.*, **145**, 1–13.

Rust, B.R. (1978) Depositional models of braided alluvium. In: *Fluvial Sedimentology* (Ed. by A.D. Mial), *Can. Soc. Petrol. Geol. Mem.* **5**, 605–626.

Sakai, H. (1989) Rifting of the Gondwanaland and uplifting of the Himalayas recorded in Mesozoic and Tertiary fluvial sediments in the Nepal Himalayas. In: *Sedimentary Facies in the Active Plate Margin* (Ed. by A. Taira & F. Masuda), pp. 723–732. Terra Scientific Publishing Company, Tokyo.

Searle, M.P. (1983) Stratigraphy, structure and evolution of the Tibetan-Tethys zone in Zanskar and the Indus suture zone in the Ladakh Himalaya. *Trans. R. Soc. Edin.: Earth Sci.*, **73**, 205–219.

Searle, M., Corfield, R.I., Stephenson, B. & McCarron, J. (1997) Structure of the North Indian continental margin in the Ladakh–Zanskar Himalayas: implications for the timing of obduction of the Spontang ophiolite, India–Asia collision and deformation events in the Himalaya. *Geol. Mag.*, **134**, 297–316.

Searle, M.P. & Rex, A.J. (1989) Thermal model for the Zanskar Himalaya. *J. Metamorp. Geol.*, **7**, 127–134.

Sinclair, H.D. (1997) Tectonostratigraphic model for underfilled peripheral foreland basins: an Alpine perspective. *Geol. Soc. Am. Bull.*, **109**, 324–346.

Sinclair, H.D. & Allen, P.A. (1992) Vertical versus horizontal motions in the Alpine orogenic wedge: stratigraphic response in the foreland basin. *Basin Res.*, **4**, 215–232.

Sinclair, H.D., Coakley, B.J., Allen, P.A. & Watts, A.B. (1991) Simulation of foreland basin stratigraphy using a diffusion model of mountain belt uplift and erosion: an example from the Central Alps, Switzerland. *Tectonics*, **10**, 599–620.

Singh, I.B. (1978) On some sedimentological and palaeoecological aspects of the Subathu-Dagshai-Kasauli succession of Simla Hills. *J. Palaeontol. Soc. India*, 19–28.

Singh, H.P. & Khanna, A.K. (1980) Palynology of the Palaeogene marginal sediments of Himachal Pradesh, India. Proceedings of the IVth International Palynological Conference, Lucknow, Vol. 1, pp. 462–471.

Singh, B.P. & Singh, H. (1995) Evidence of tidal influence in the Murree Group of rocks of Jammu Himalaya, India. In: *Tidal Signatures in Modern and Ancient Sediments* (Ed. by B.W. Flemming & A. Bartholoma), *Spec. Publ. Int. Assoc. Sedimentol.* **24**, 343–351.

Srikantia, S.V. & Bhargava, O.N. (1967) Kakara series: a new Palaeocene Formation in Simla Hills. *Bull. Geol. Soc. India*, **4**, 114–116.

Srikantia, S.V. & Sharma, R.P. (1970) The occurrence of rocks of Kakara (Palaeocene) affinity in the Bakhalag–Bughar belt, Himachal Pradesh. *J. Geol. Soc. India*, **11**, 185–188.

Srivastava, V.K. & Casshyap, S.M. (1983) Evolution of the pre-Siwalik Tertiary basin of Himachal Himalaya. *J. Geol. Soc. India*, **24**, 134–147.

Srivastava, P. & Mitra, G. (1994) Thrust geometries and deep structure of the outer and lesser Himalaya, Kumaun and Garhwal (India): implications for evolution of the Himalayan fold-and-thrust belt. *Tectonics*, **13**, 89–109.

Staubli, A. (1989) Polyphase metamorphism and the development of the Main Central Thrust. *J. Metamorph. Geol.*, **7**, 73–93.

Tagami, T., Galbraith, R.F., Yamada, G.M. & Laslett, G.M. (1998) Revised annealing kinetics of fission-tracks in zircon and geological implications. In: *Advances in Fission-track Geochronology* (Ed. by P. Van den Haute & F. DeCorte), pp. 99–112. Kluwer Academic Press, Amsterdam.

Thakur, V.C. (1998) Structure of the Chamba nappe and position of the Main Central Thrust in Kashmir Himalaya. *J. Asian Earth Sci.*, **16**, 269–282.

Treloar, P. & Searle, M.P. (eds) (1993) *Himalayan Tectonics*, Geological Society Special Publication 74, 630pp. Bath, UK.

Valdiya, K.S. (1980) *Geology of Kumaun Lesser Himalaya*. Wadia Institute of Himalayan Geology, Dehra Dun, India, 291pp.

Valdiya, K.S. & Bhatia, S.B. (eds) (1980) *Stratigraphy and Correlations of Lesser Himalayan Formations*. Hindustan Publishing Corporation, India, 330pp.

Vance, D. & Harris, N. (1999) Timing of prograde metamorphism in the Zanskar Himalaya. *Geology*, **27**, 395–398.

Von Blanckenburg, F. & Davies, J.H. (1995) Slab breakoff: a model for syncollisional magmatism and tectonics in the Alps. *Tectonics*, **14**, 120–131.

Wadia, D.N. (1975) *Geology of India*. Tata McGraw-Hill Publishing Company Ltd, New Delhi, 508pp.

Weber, K. (1972a) Notes on the determination of illite crystallinity. *Neues Jahrb. Mineral. Monatsh.*, **6**, 267–276.

Weber, K. (1972b) Kristallinitat des illites in Tonschiefern und andere kriterien schwacher metamorphose im nordost-lichen Rheinischen Schiefergebirge. *Neues Jahrb. Palaeontol. Abh.*, **141**, 333–363.

White, N., Parrish, R.R., Bickle, M.J., Najman, Y.M.R., Burbank, D. & Maithani, A. (2001) Metamorphism and exhumation of the northwest Himalaya constrained by U–Th–Pb analysis of detrital monazite grains from early foreland basin sediments. *J. Geol. Soc. London*, **158**, 625–635.

White, N.M., Pringle, M.S., Garzanti, E., Bickle, M.J., Najman, Y.M.R., Chapman, H. & Friend, P. (2002) Constraints on the exhumation and erosion of the High Himalayan Slab, NW India, from foreland basin deposits. *Earth Planet. Sci. Lett.*, **195**, 29–44.

Willis, B. (1993a) Ancient river systems in the Himalayan foredeep, Chinji Village area, northern Pakistan. *Sediment. Geol.*, **88**, 1–76.

Willis, B. (1993b) Evolution of Miocene fluvial systems in the Himalayan foredeep through a two kilometer-thick succession in northern Pakistan. *Sediment. Geol.*, **88**, 77–121.

Manuscript accepted: 23 May 2003

